Mitigating traffic congestion induced by Transportation Network Companies: a policy analysis

Kenan Zhang¹ and Yu (Marco) Nie *1

¹Department of Civil and Environmental Engineering, Northwestern University 2145 Sheridan Road, Evanston, IL 60208, USA

October 30, 2022

Abstract

This paper analyzes and evaluates several policies aiming to mitigate the congestion effect a Transportation Network Company (TNC) brings to bear on an idealized city that contains a dense central core surrounded by a larger periphery. The TNC offers both solo and pooling ehail services to the users of public transport. We develop a spatial market equilibrium model over two building blocks: an aggregate congestion model that describes the traffic impact of TNC operations on all travelers in the city, including private motorists, and a matching model that estimates the TNC's level of service based on the interactions between riders and TNC drivers. Based on the equilibrium model, we formulate and solve the optimal pricing problem, in which the TNC seeks to optimize its profit or social welfare subject to regulatory costs and/or constraints. Three congestion mitigation policies are implemented in this study: (i) a trip-based policy that charges a congestion fee on each solo trip starting or ending in the city center; (ii) a cordon-based policy that charges TNC vehicles entering the city center with zero or one passenger; and (iii) a cruising cap policy that requires the TNC to maintain the fleet utilization ratio in the city center above a threshold. Based on a case study of Chicago, we find TNC operations may have a significant congestion effect. Failing to anticipate this effect in the pricing problem leads to sub-optimal decisions that worsen traffic congestion and hurt the TNC's profitability. Of the three policies, the trip-based policy delivers the best performance. It reduces traffic congestion modestly, keeps the TNC's level of service almost intact, and improves overall social welfare substantially. The cruising cap policy benefits private motorists, thanks to the extra congestion relief it brings about. However, because other stakeholders together suffer a much greater loss, its net impact on social welfare is negative. Paradoxically, the policy could worsen the very traffic conditions in the city center that it is designed to improve.

Keywords: transportation network company; e-hail; pooling; spatial equilibrium; congestion mitigation policy

^{*}Corresponding author, E-mail: y-nie@northwestern.edu; Phone: 1-847-467-0502.

1 Introduction

The ride-hail industry has gone through a significant transition phase in the past decade, largely driven by the rapid growth of transportation network companies (TNCs) such as Uber and Lyft (Taylor et al., 2016; Rayle et al., 2016; Clewlow and Mishra, 2017). While the e-hail service offered by TNCs is widely credited for boosting productivity and enhancing level of service (Cramer and Krueger, 2016), its adverse traffic impact in already-congested city centers has drawn increased scrutiny. In New York City, the average traffic speed dropped 15% from 2013 to 2017, a decline accompanied by a 36% increase in vehicle miles traveled (VMT) and an 81% increase in vacant vehicle hours for all ride-hail vehicles (taxis and TNC vehicles) (Schaller, 2017a). The lion share of the extra traffic was no doubt contributed by TNC vehicles, as the market share of taxis has shrunk precipitately in the same period. By simulating a counterfactual scenario without TNCs, Erhardt et al. (2019) estimate that TNCs might have added 40% additional vehicle hours in weekdays in San Francisco from 2010 to 2016.

As similar empirical evidence piles on (e.g., Schaller, 2017b, 2018a; Henao, 2017; NASEM, 2021), several cities started to consider policy initiatives aiming to mitigate the traffic impact induced by excessive TNC operations. For instance, New York City now charges \$2.75 on each TNC trip that passes through a designated congestion zone (south of 96th Street in Manhattan) with only one passenger.¹ The charge is reduced to \$0.75 if the trip is pooled (i.e., shared by at least two passengers). Similarly, Chicago charges \$3.00 for each solo trip (\$1.25 for each pooling trip) that starts or ends inside its downtown area². In 2019, San Francisco enacted a TNC tax, which imposed a 3.25% surcharge on all solo trips and a 1.5% surcharge on all pooling trips³. Besides these trip-based congestion mitigation policies, directly regulating the occupancy rate of TNC vehicles has also been proposed (see e.g., Schaller, 2017a). Here, the target is the cruising time that is often seen as a counterproductive dead-weight loss from the vintage point of a city manager. Another option is to piggyback on exist congestion pricing schemes. Li et al. (2020) examine cordon-based pricing (see e.g. de Palma and Lindsey, 2011) in the context of regulating the ride-hail market. Unlike trip-based schemes, cordon-based pricing levies a toll on every vehicle, vacant or not, entering a congested area encircled by a cordon line.

Given TNCs' expanding footprint around the world, it is likely that we are just witnessing the beginning of regulatory actions targeting the traffic havoc wrought by them. City managers will need to understand the full impact of these actions, not only on traffic congestion, but also on the welfare of all stakeholders in the urban transport system: riders, drivers, TNCs and other travelers. The purpose of this study is to support such policy analysis by developing a model that captures the complex interactions among various stakeholders. More specifically, we would like to address the following questions: (i) do TNC operations have an outsized traffic impact, as suggested by the empirical studies? (ii) if so, should TNCs take it into account as they design operational strategies? and (iii) which regulatory policies mitigate the impact more effectively?

Our model includes several features critical to the intended analysis, which, to the best of our knowledge, have not been satisfactorily integrated in the literature. First, it incorporates both solo

¹See https://www.tax.ny.gov/bus/cs/csidx.htm

²See https://www.chicago.gov/city/en/depts/bacp/supp_info/city_of_chicago_congestion_pricing.html

 $^{^3}$ See https://www.governing.com/news/headlines/San-Francisco-Will-Increase-Taxes-for-Ride-Hailing-Trips.html

and pooling rides, and represents their operational characteristics based on the spatial matching model developed in Zhang and Nie (2021). As seen above, most congestion mitigation policies recognize the importance of distinguishing pooling trips from solo trips, because ridesharing is widely considered a low-cost and effective travel demand management strategy (Shaheen, 2018)⁴ Second, the idea of a managed congestion zone makes modeling spatial heterogeneity a necessity. At the minimum, one must separate the trips inside the zone from the outside. In this study, we consider two zones connected by arterial roads: one representing the city center and the other the peripheral area. Third, given the focus on congestion mitigation, we model the congestion effect based on macroscopic traffic flow theories. Specifically, the travel speed of TNC vehicles within and between zones is allowed to vary with the total VMT they generate.

In the proposed model, a single TNC platform offers both solo and pooling e-hail services to passengers traveling within and between the two zones. Thus, there are four market segments, two intra-zonal and two inter-zonal. On the demand side, utility-maximizing travelers choose between transit and ride-hail (solo or pooling). In other words, the share of all other modes (e.g., driving, walking), hence their contribution to traffic congestion, is held fixed and exogenous in the model. This simplification allows us to focus on the competition between transit, solo rides, and pooling rides, which is affected by the congestion mitigation policies the most. On the supply side, drivers' decision to work for the platform depends on the average earning promised by the job. The platform aims to maximize its profit by pricing solo and pooling rides in each of the four market segments, as well as setting drivers' compensation rate. While making these decisions, it must anticipate their effects on travelers' mode choice and drivers' participation through a market equilibrium model, along with the possible change in the travel speed of its fleet.

Using the above model, we analyze and compare three congestion mitigation policies. The first policy is inspired by the trip-based fee recently implemented in New York City and Chicago. It charges a flat congestion fee on each solo trip starting or ending in the city center. For simplicity, pooling trips are exempted from this policy. In the second policy, TNC vehicles must pay a flat congestion fee each time they *enter* the city center. This fee is only waived if the vehicle is serving a pooling trip. The third policy imposes a cruising cap in the city center. Under this policy, the platform must ensure the average occupancy rate of its fleet no less than a target threshold. A similar policy was proposed in New York City in 2019, though shortly struck down (Guse, 2019).

The rest of this paper is organized as follows. A brief review on related work is presented in Section 2. Section 3 details the congestion and matching model in the spatial ride-hail market. The equilibrium model and the platform's pricing problem are presented in Section 4 and Section 5, respectively. The three congestion mitigation policies are introduced in Section 6, and Section 7 reports numerical results. Finally, Section 8 summarizes the main findings and provides several directions for future research.

⁴It is important to note the success of pooling service largely depends on high demand density (Zhang and Nie, 2021), which explains why such services are available and viable only in densely populated urban areas. The impact of pooling need not always be positive either. Recent studies show it could instead increase the total VMT due to the extra detours and the induced demand that would otherwise choose "greener" modes such as transit and biking (Schaller, 2018a, 2021). Hence, pooling trips should be regulated as well as regular e-hail trips, although differential treatments may be necessary.

2 Related work

Studies of the ride-hail market have grown rapidly in multiple fronts, from designing matching mechanisms (e.g., Zhang et al., 2019; Özkan and Ward, 2020), optimizing pricing strategies (e.g., Banerjee et al., 2015; Cachon et al., 2017; Zha et al., 2018; Bimpikis et al., 2019), to rebalancing vacant vehicles (e.g., Zhang and Pavone, 2016; Braverman et al., 2019). The reader is referred to Wang and Yang (2019) for a recent survey. Here we are focused on the equilibrium analysis (Section 2.1), congestion management (Section 2.2), and regulations (Section 2.3) of the ride-hail market.

2.1 Equilibrium analysis of ride-hail market

The equilibrium analysis of the taxi market dates back to 1970s. We highlight two representative studies, Douglas (1972) and Arnott (1996), which respectively model street-cruising and radio-dispatch taxi services at an aggregate level. The two studies both identify a salient feature of ride-hail service—the friction in matching passengers with drivers in space. In a street-cruising mode, passengers and drivers do not know the exact location of each other, so a considerable amount of time must be consumed in searching/waiting. While searching is no longer an issue in radio-dispatch mode, passengers still need to wait when the vehicle is en-route to pick up them at the trip origin. In both cases, the matching friction prevents passengers from being picked up right away. The ensued wait time then becomes a primary measure of level-of-service (LOS).

Yang and Wong (1998) propose the first networked taxi model that considers the movements of taxi drivers between different zones. A number of follow-up studies extend the model to consider congestion effects, elastic demand, and passenger and vehicle heterogeneity (e.g., Wong et al., 2001, 2008). Yang et al. (2010) introduce explicit matching friction in the form of Cobb-Douglas production function, which describes the relationship between waiting passengers, vacant vehicles and pickup rate. More recent studies apply other types of matching functions, such as the urn-ball matching function (e.g., Shapiro, 2018; Buchholz, 2019) and empirical functions constructed from simulations (e.g., Frechette et al., 2019). Another line of work attempts to apply the networked taxi model to study the emerging e-hail services provided by TNCs (e.g., Zha et al., 2016; Wang et al., 2016).

Castillo et al. (2018) show e-hail service may be trapped in an inefficient state called *Wild Goose Chase* (WGC). When most vacant vehicles are stuck in the pickup phase, very few vehicles are available for new passengers, leading to extensively long wait times. Xu et al. (2020) examine the same phenomenon and derive a supply function from a double-ended queuing model. They show that the system is prone to WGC if the platform adopts a fixed matching radius. Notably, taxi service is not subject to the WGC trap, precisely because its antiquated matching technology prevents it from over-committing supply to the pickup phase. Inspired by the discrepancy, Zhang et al. (2019) propose a general spatial matching model that unifies the matching mechanisms of both street-cruising taxi and e-hail. The model predicts e-hail loses economies of scale enjoyed by street-hailing taxi, albeit it holds an overwhelming advantage in terms of total factor productivity in matching. The result is validated using empirical data.

While various equilibrium models have been employed to study e-hail market, only a few have considered ride-pooling. To the best of our knowledge, all of them rely on aggregate

models. Zhang and Nie (2021) extend the spatial matching model developed in Zhang et al. (2019) to accommodate pooling. They limit the number of participants of any pooling ride to two, and explicitly model the pickup detour as a function of the pooling demand. The results from their case study of Chicago indicate that providing both solo and pooling rides is a dominant strategy for TNCs. Yan et al. (2019) propose a ride-pooling model based on the concept of dynamic waiting. In their model, a pooling passenger first waits for a predefined time to find a match. If a pooling partner is found within the time window, the two are picked up and dropped off at the midpoint of their origins and destinations; otherwise, the passenger is given a solo ride. The authors find a joint implementation of dynamic pricing and dynamic waiting increases both vehicle utilization and trip production, while reducing price volatility. Ke et al. (2020a) propose to treat the probability of successfully finding a pooling match as an increasing function of pooling demand and matching interval. In a sequel, Ke et al. (2020b) explore the impact of ride-pooling on traffic congestion. Their analysis shows (i) under certain conditions, pooling could help reduce the travel time of both ride-hail passengers and private vehicle drivers, and (ii) the matching interval in pooling is critical to achieving such a win-win outcome. Like Zhang and Nie (2021), Vignon et al. (2021) consider a joint operation of solo and pooling services. They also analyze congestion externality using a macroscopic traffic flow model.

2.2 Congestion pricing

Traffic congestion is a long-standing issue in densely populated metropolitan areas. INRIX estimates congestion costed the United States \$88 billion a year in terms of wasted time and fuel, and, on average, each driver lost about 100 hours to traffic jam (INRIX Research, 2019). The real damage is likely far greater since the estimate leaves out the cost of greenhouse gas emissions and air pollution. From an economic point of view, excessive traffic congestion is caused by travel externality, a cost imposed by a marginal traveler on the system but not included in their own travel utility (de Palma and Lindsey, 2011). One possible approach to "internalizing" the cost of such externality is congestion pricing, i.e., charging travelers a congestion toll (Pigou, 1920). This idea has been extensively examined by economists, engineers and planners alike in the last century. The resulting policies have attempted to tie the congestion toll to travel distance (e.g., Goodin et al., 2009), congested road segments (e.g., Verhoef et al., 1996; Verhoef, 2002), access to a congested zone (e.g., De Palma et al., 2005; Maruyama and Sumalee, 2007) and crossing of predefined cordon-lines (e.g., Zhang and Yang, 2004; Ho et al., 2005; Mun et al., 2005).

As TNCs' traffic impact draws public attention, researchers began to contemplate congestion pricing targeting their operations. Schaller (2018b) suggests a surcharge of \$50/hour in Midtown and \$20/hour in the other congested areas of Manhattan on ride-hail vehicles, which is expected to result in an 8% drop in the demand for ride-hail and a 30% decrease in VMT. Li et al. (2021) suggest imposing a congestion fee, either by trip or based on operation time, and combining it with a minimum wage policy. Their numerical experiments show that, although both pricing schemes reduce ride-hail demand, the time-based pricing can more effectively improve vehicle occupancy. Using a spatial market equilibrium model, Li et al. (2020) compare three congestion pricing policies: (i) uni-directional cordon fee, (ii) bi-directional cordon fee, and (iii) trip-based fee. They find all three policies can reduce vacant vehicle density in the congested area and increase vehicle occupancy across the entire market. However, uni-directional cordon pricing also

improves service quality outside the congested area and is more effective in reducing congestion.

2.3 Regulations on TNCs

Since the time when TNCs first caught the attention of the world, the debate on whether and how to regulate them has started. As a direct competitor, the taxi service has always been tightly regulated in terms of both trip fare and market entry. However, TNCs are a tougher case to crack for regulators, largely due to their peculiar labor structure. TNCs insist their drivers are not employees, but rather "independent contractors" who work at their will and thus voluntarily forgo standard labor protections. This claim has been contested nationally and internationally, although for now it is upheld by Proposition 22 in California (CNN Business, 2020). A much debated issue concerns whether the minimum wage law should cover TNC drivers, regardless of their employment status. The advocates point out that setting a minimum wage could ensure a thicker market that promises better service quality, which benefits both passengers and drivers (Parrott and Reich, 2018; Li et al., 2019). The opponents argue such benefits may only be shortlived, because TNCs will respond to the minimum-wage policy by restricting the entry of drivers into their supply reservoir (Gurvich et al., 2019; Asadpour et al., 2019). Furthermore, if both solo and pooling are offered, the minimum wage policy may force a profit-maximizing platform to discourage pooling, so as to absorb the extra vehicle supply induced by an artificially high minimum wage (Zhang and Nie, 2021).

Other policy instruments are also discussed in the literature. Zha et al. (2016) show that a cap on the commission rate (the fraction of trip fare taken by TNCs) is sufficient to guarantee a second-best outcome. This finding is further confirmed in Vignon et al. (2021), which incorporates both pooling and congestion externality. Specifically, they find a commission cap imposed on solo rides, along with a congestion toll charged on drivers, could achieve a second-best outcome. Further, the toll can be replaced by congestion fees on both solo and pooling trips at different rates. Yu et al. (2020) study the entry control policy of TNC vehicles in a market where they compete against taxis for passengers. The results show a well-designed control policy can improve social welfare while achieving a satisfactory balance among several competing objectives. NASEM (2021) offers a series of policy recommendations to public transit agencies and local authorities. Among them, congestion pricing on ride-hail trips and incentives on pooling are emphasized.

3 A spatial ride-hail model

Consider a city that consists of two zones: a central business district (CBD) and a peripheral area (PA), as shown in Figure 1(a). Four types of trips could take place in such a city: *central trips* that start and end within CBD, *peripheral trips* that start and end within PA, *inbound trips* that start in PA and end in CBD, and *outbound trips* that start in CBD and end in PA. Assume that, for each market segment, the origins and destinations of all trips are uniformly distributed in the respective zones. Also, we assume a fixed portion of travelers drive alone, and the rest choose between transit and ride-hail service provided by a TNC platform (*platform* hereafter) that monopolizes the market. Here, transit is considered the only alternative to ride-hail because it

is widely considered a genuine competitor in the literature.⁵ The platform offers both solo and pooling rides that may be priced differently. Thus, travelers opting out driving must choose from a set of three modes, denoted as $\mathcal{M} = \{s, p, t\}$, where s, p and t refers to solo, pooling and transit, respectively.

Assumption 1 For each pooling ride, a passenger is shared with one and only one passenger. Besides, each pooling ride starts when both passengers are on-board. Hence, each pooling ride contributes to half a unit vehicle flow in the market equilibrium model.

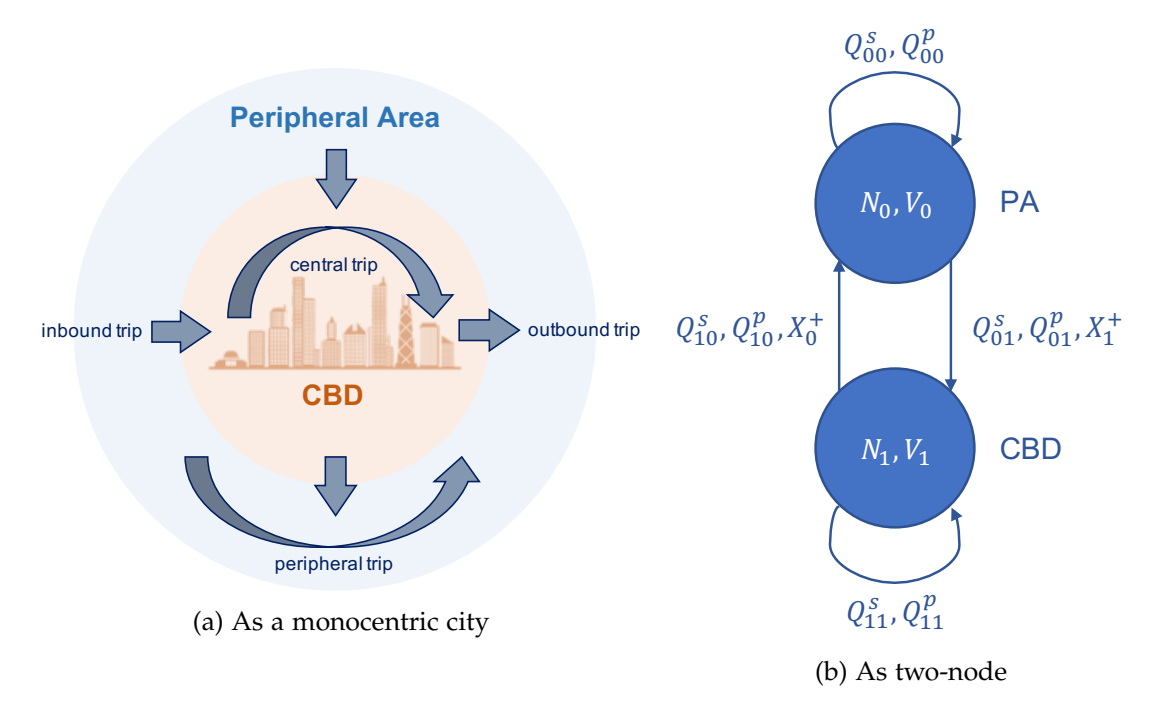


Figure 1: Illustration of the spatial ride-hail market.

For easy reference, we shall index PA and CBD as 0 and 1, and denote the set of zone indices as $\mathcal{I} := \{0,1\}$. We abstract the city as a network of two zones connected by arterial roads, as illustrated Figure 1(b). Let D_{ij}^0 denote the total demand for all public modes included in \mathcal{M} from zone i to zone j. We use Q_{ij}^m to denote the demand for each mode $m \in \mathcal{M}$ and thus

$$D_{ij}^{0} = \sum_{m \in \mathcal{M}} Q_{ij}^{m}, \quad i, j \in \mathcal{I}.$$

$$\tag{1}$$

At a stationary state, if there are more occupied vehicles (i.e., with passengers) leaving a zone than those entering it, there must be vehicles relocating to the zone *without* passengers. We define the net loss of occupied vehicles in zone *i* as the inflow of occupied vehicles less the outflow of occupied vehicles. Mathematically, it is given by

$$X_{i} = \left(Q_{ij}^{s} + \frac{1}{2}Q_{ij}^{p}\right) - \left(Q_{ji}^{s} + \frac{1}{2}Q_{ji}^{p}\right), \quad i, j \in \mathcal{I}; \ i \neq j.$$
 (2)

⁵The modeling framework is flexible enough to accommodate active travel modes such as biking or scooting. Yet, they may not be viable for most ride-hail trips in term of both distance and availability.

In Eq. (2), each pooling ride contributes to half a unit vehicle flow as per Assumption 1. Accordingly, the amount of vehicle flows needed to make up the loss in zone i is given by $X_i^+ = \max(0, X_i)$, referred to as the relocation vehicle flow of zone i.

For a given analysis period, the total vehicle operation time equals the number of vehicles in the local market associated with zone i, denoted as N_i , times the length of the period. We shall normalize the length to 1 for simplicity. The total vehicle time consists of four parts: (i) the occupied time inside zone i, i.e., the time spent to deliver passengers on trips both starting and ending in zone i, (ii) the occupied time from zone i to the other zone, (iii) the vacant time spent in searching passengers inside zone i, and (iv) the vacant time spent in relocating from the other zone to zone i. Accordingly, the conservation of total vehicle time of zone i dictates

$$N_{i} = \sum_{j' \in \mathcal{I}} Q_{ij'}^{s} \tau_{ij'}^{s} + \frac{1}{2} \sum_{j' \in \mathcal{I}} Q_{ij'}^{p} \tau_{ij'}^{p} + V_{i} + X_{i}^{+} \tau_{ji}^{r}, \quad i \in \mathcal{I}; \ i, j \neq j,$$
(3)

where V_i is the vacant vehicle time in zone i, $\tau_{ij'}^s$ and $\tau_{ij'}^p$ are the average trip duration of solo and pooing rides from zone i to zone j', and τ_{ii}^r denotes the relocation time from zone j to zone i.

In what follows, Section 3.1 proposes a congestion model that links the trip duration and relocation time (i.e., τ_{ij}^m , $m \in \{s, p, r\}$) to ride-hail vehicle flows. Section 3.2 presents the spatial matching model adopted to estimate average passenger wait times for both solo and pooling rides. Both the travel and wait time affect the demand for ride-hail services, as explained in Section 4. All notations used in this study are summarized in Appendix A.

3.1 Congestion model

Let d_{ij}^m , $m \in \{s, p\}$ denote the average trip distance for mode m from zone i to zone j. Similarly, we define the average relocation distance as d_{ij}^r . The travel times are then given as

$$\tau_{ij}^s = d_{ij}^s / v_{ij} + \varepsilon_s, \quad i, j \in \mathcal{I}, \tag{4a}$$

$$\tau_{ij}^p = d_{ij}^p / v_{ij} + \varepsilon_p, \quad i, j \in \mathcal{I}, \tag{4b}$$

$$\tau_{ij}^r = d_{ij}^r / v_{ij}, \qquad i, j \in \mathcal{I}; \ i \neq j, \tag{4c}$$

where ε_s and ε_p are additional travel time independent of trip distance and the matching process (e.g., the time spent in finding the TNC vehicle at the pickup location and the drop-off time). We assume $d_{ij}^p > d_{ij}^s$ because of the detour required to visit two destinations in pooling rides (the detour at the origin is captured in wait time, see Section 3.2). While the en-route detour $d_{ij}^p - d_{ij}^s$ is expected to vary with pooling demand (Ke et al., 2021), we have shown the market equilibrium is generally insensitive to the impact of such dependency (Zhang and Nie, 2021). Hence, we shall treat d_{ij}^m as exogenous and calibrate them from empirical data (see Appendix B). Similarly, ε_p and ε_s (with $\varepsilon_p > \varepsilon_s$) are also estimated from data.

We use Greenshields' fundamental diagram (Greenshields et al., 1935) and BPR function (US Bureau of Public Roads, 1964) to represent the dependence of speed on traffic within and between zones, respectively. Let v_f be the free-flow speed, $\rho_i^{\rm jam}$ be the jam density in zone i, and C_p be an aggregate road capacity between the two zones. The intra- and inter-zonal speeds are given by

Intra-zone:
$$v_{ii} = v_f \left(1 - \frac{\rho_i + \bar{\rho}_i}{\rho_i^{\text{jam}}} \right),$$
 $i \in \mathcal{I},$ (5a)

Inter-zone:
$$v_{ij} = v_f \left[1 + 0.15 \left(\frac{z_{ij} + \bar{z}_{ij}}{C_p} \right)^4 \right]^{-1}$$
, $i, j \in \mathcal{I}; i \neq j$, (5b)

where ρ_i ($\bar{\rho}_i$) is the ride-hail vehicle (background traffic) density in zone i and z_{ij} (\bar{z}_{ij}) the ride-hail (background traffic vehicle flow from zone i to zone j. Note that all background traffic is produced by private motorists (i.e., those who do not choose any of the three public modes). Using historical traffic and TNC data, we may calibrate the parameters used in Eq. (5) and estimate the magnitude of background traffic (i.e., $\bar{\rho}_i$ and \bar{z}_{ij}). More details are included in Appendix B.

We end this section by noting that pick-up and drop-off maneuvers could induce additional congestion as they may block other traffic (Goodchild et al., 2019; Liu et al., 2020). The magnitude of this effect depends on factors like road design, built environment, and prevailing traffic conditions. Properly endogenizing this effect may require a model with much more granular representation of the urban road network, which is beyond the scope of the present study.

3.2 Matching model

The *matching process* covers the time period from the moment when passengers send a ride request to the platform to the moment a matched vehicle starts the trip with all assigned passengers on board. It consists of a dispatching phase that assigns requests to a suitable vehicle, and a pickup phase during which the assigned vehicle is en-route to pick up the passengers. Following Zhang and Nie (2021), we assume all pooling passengers are paired in the dispatching phase. Although this assumption seems strong and excludes the possibility of en-route pooling, it captures the main trade-off in pooling while maintaining tractability. Accordingly, for each pooling ride, the pickup phase is further divided into two sub-phases. In the first sub-phase, the vehicle picks up the closer passenger, and in the second, it takes a "detour" to get the other passenger. Therefore, both passengers are subject to the same wait time, which equals the duration of the matching process.

Following Zhang and Nie (2021), we estimate the mode- and market-specific wait time without explicitly differentiating the pickup phase from the dispatching phase. Note that the duration of the latter is usually much shorter than that of the former (Zha et al., 2018), regardless of the dispatching policy (Castillo et al., 2018; Yang et al., 2020).

Let w_{ij}^m , $m \in \{s, p\}$ be passenger wait time of mode m for the market segment ij. To derive closed-form formula for w_{ij}^m , we introduce two assumptions. First, we assume vacant vehicles and waiting passengers are both uniformly distributed in each zone. While it may not always hold in reality (passenger and drivers do sometimes tend to concentrate around "hot spots"), this assumption allows us to capture the interaction between passenger demand and vehicle supply in the matching process while retaining analytical tractability. Second, we assume passengers are only matched with vehicles in the same zone and pooling passengers share the same origin and destination zones. This helps exclude complexities involved in inter-zonal pooling, which is unlikely to happen anyway given the geographical scale of zones defined in this study. The two assumptions are formally stated as follows:

Assumption 2 The vacant vehicles and the waiting passengers in each local market are uniformly distributed in space. Passengers keep waiting at the same location prior to pickup.

Assumption 3 A ride-hail passenger can only be picked up by a vacant vehicle in the same zone and pooling passengers must share the same origin and destination zone.

With the above assumptions, the wait time in zone i can be represented as a function of the vacant vehicle density in zone i, denoted as Λ_i , and the densities of passengers waiting for solo and pooling rides from zone i to zone j, denoted as Π_{ij}^s and Π_{ij}^p , respectively. The formula are given as follows (see Zhang and Nie (2021) for details):

$$w_{ij}^s = \frac{\delta}{2v_{ii}} \sqrt{\frac{\Pi_i^{\text{eff}}}{k\Lambda_i}},$$
 $i, j \in \mathcal{I},$ (6a)

$$w_{ij}^p \simeq w_{ij}^s \sqrt{\frac{\kappa + 4b\Pi_{ij}^p}{2\kappa + 4b\Pi_{ij}^p}} + \frac{\delta}{2v_{ii}} \frac{1}{\sqrt{b\Pi_{ij}^p}}, \quad i, j \in \mathcal{I},$$
 (6b)

where

- $\Pi_i^{\text{eff}} = \sum_j \left(\Pi_{ij}^s + \frac{1}{2} \Pi_{ij}^p \right)$ is the effective waiting passenger density in zone i;
- The parameter δ is the detour ratio of the road network (Boscoe et al., 2012; Yang et al., 2018), defined as the ratio between the distance of the actual travel path and the line distance between two points in the network;
- The parameters *k* and *b* measure the matching efficiency between vehicles and passengers, and between pooling passengers, respectively⁶;
- The parameter κ is related to the approximations made when deriving w_p .

Since no variable is subscripted with j in Eq. (6a), we have $w_{ii}^s = w_{ij}^s$ for $i, j \in \mathcal{I}$; $i \neq j$. In Eq. (6b), the first term gives the duration of dispatching phase plus the pickup phase of the first passenger, while the second is the detour time to pick up the second passenger.

4 Market equilibrium

In this section, we first explain how the demand and supply sides are set up and then present a fixed-point formulation of the spatial market equilibrium.

4.1 Demand and supply

The mode choice is governed by the generalized cost of the three modes. For a trip from zone i to zone j, the generalized costs are computed as

Solo:
$$u_{ij}^s = f_{ij}^s + v(w_{ij}^s + \tau_{ij}^s), \qquad i, j \in \mathcal{I},$$
 (7a)

Pooling:
$$u_{ij}^{p} = f_{ij}^{p} + \nu(w_{ij}^{p} + \tau_{ij}^{p}) + \zeta^{p}, \quad i, j \in \mathcal{I},$$
 (7b)

 $^{^6}$ The reader is referred to Zhang and Nie (2021) for the formal definition of k, b and discussions on why they can be treated as exogenous.

Transit:
$$u_{ij}^t = f_{ij}^t + \nu \tau_{ij}^t + \zeta^t$$
, $i, j \in \mathcal{I}$, (7c)

where f_{ij}^m is the trip fare of mode $m \in \mathcal{M}$, ν is the value of time, τ_{ij}^t denotes the transit travel time, and ζ^p , ζ^t represent the exogenous disutility of pooling and transit attributed to lack of privacy, discomfort, crowdedness, etc. Here, we assume the transit speed is free of congestion and thus τ_{ij}^t remains constant. The transit trip fare is also set to be fixed and thus the generalized cost of transit is a constant.

Recall that the total demand from zone i to zone j is D^0_{ij} . We model the share of each mode with a continuous and differentiable function of the generalized costs, denoted as $q: \mathbb{R}^3 \to (0,1)$. Then, the demand for mode $m \in \mathcal{M}$ is given by

$$Q_{ij}^{m} = D_{ij}^{0} q(u_{ij}^{m}, \mathbf{u}_{ij}^{-m}), \quad i, j \in \mathcal{I},$$
(8)

where \mathbf{u}_{ij}^{-m} , $-m := \mathcal{M} \setminus \{m\}$ refers to the generalized cost of modes other than m. Without loss of generality, we assume $\partial Q_{ij}^m/\partial \mathbf{u}_{ij}^m < 0$ and $\partial Q_{ij}^m/\partial \mathbf{u}_{ij}^{-m} > 0$, that is, the passenger demand for mode m between a given OD pair decreases with the cost of mode m but increases with the costs of other modes.

As for the vehicle supply, we assume drivers can freely enter (exit) the market if and only if the expected earning of ride-hail service is higher (lower) than their reservation rate (i.e., the earning of the alternative employment opportunity). This assumption aligns with the finding of recent studies on the labor supply of ride-hail services that drivers exhibit a positive wage elasticity (e.g., Angrist et al., 2017; Chen and Sheldon, 2016; Sun et al., 2019).

Let e be the expected ride-hail earning rate and assume drivers' reservation rate \tilde{e}_0 follows a probability distribution with a cumulative distribution function (CDF) $g(\cdot)$. Thus, $g(\cdot)$ captures the variations in drivers' alternative employment opportunities and it may be constructed from the income data associated with those opportunities. Then, the number of drivers entering the market is given by

$$N = \sum_{i \in \mathcal{I}} N_i = S_0 Pr(\tilde{e}_0 \le e) = S_0 g(e), \tag{9}$$

where *N* denotes the total number of drivers entering the market.

The platform pays drivers at the compensation rate η per unit occupied time, regardless of whether they serve solo or pooling trips.⁷ At equilibrium, drivers are distributed between the two zones such that the average earning rates are identical. In the absence of any regulatory interventions (e.g., congestion pricing), the average earning rate is computed as

$$e = \frac{\eta}{N_i} \sum_{i \in \mathcal{I}} \left(Q_{ij}^s \tau_{ij}^s + \frac{1}{2} Q_{ij}^p \tau_{ij}^p \right), \quad i \in \mathcal{I}.$$
 (10)

4.2 Fixed-point formulation

We are now ready to establish the market equilibrium under a pricing strategy (\mathbf{f}_s , \mathbf{f}_p , η). For an analysis period normalized to a unit length (say an hour), the equilibrium is characterized by the following system of equations:

⁷In practice, a small fee is often offered to drivers for each additional pickup in pooling trips. Yet, Zhang and Nie (2021) find the system performance is insensitive to such a pickup fee. Hence, it is omitted in this study for simplicity.

Mode choice:
$$Q_{ij}^m = D_{ij}^0 q(u_{ij}^m; u_{ij}^{-m}),$$
 $i, j \in \mathcal{I},$ (11a)

Fleet size:
$$N = S_0 g(e)$$
, (11b)

Flow conservation:
$$N_i = V_i + \sum_{j' \in \mathcal{I}} Q^s_{ij'} \tau^s_{ij'} + \frac{1}{2} \sum_{j' \in \mathcal{I}} Q^p_{ij'} \tau^p_{ij'} + X^p_i \tau^p_{ji}, \qquad i, j \in \mathcal{I}; i \neq j,$$
 (11c)

$$X_{i} = \left(Q_{ij}^{s} + \frac{1}{2}Q_{ij}^{p}\right) - \left(Q_{ji}^{s} + \frac{1}{2}Q_{ji}^{p}\right), \qquad i, j \in \mathcal{I}; i \neq j,$$
 (11d)

Passenger density:
$$\Pi_i^{\text{eff}} = \frac{1}{A_i} \sum_{j \in \mathcal{I}} \left(Q_{ij}^s w_{ij}^s + \frac{1}{2} Q_{ij}^p w_{ij}^p \right),$$
 $i \in \mathcal{I},$ (11e)

$$\Pi_{ij}^{p} = \frac{1}{A_i} Q_{ij}^{p} w_{ij}^{p}, \qquad i, j \in \mathcal{I},$$

$$(11f)$$

Vehicle density:
$$\Lambda_i = \frac{1}{A_i} V_i$$
, $i \in \mathcal{I}$, (11g)

Wait time:
$$w_{ij}^s = \frac{\delta}{2v_{ii}} \sqrt{\frac{\Pi_i^{\text{eff}}}{k\Lambda_i}},$$
 $i, j \in \mathcal{I},$ (11h)

$$w_{ij}^p = w_{ij}^s \sqrt{\frac{\kappa + 4b\Pi_{ij}^p}{2\kappa + 4b\Pi_{ij}^p}} + \frac{\delta}{2v_{ii}} \frac{1}{\sqrt{b\Pi_{ij}^p}}, \qquad i, j \in \mathcal{I},$$
 (11i)

Traffic speed:
$$v_{ii} = v_f \left[1 - \frac{1}{\rho_i^{\text{jam}} A_i} \left(Q_{ii}^s \tau_{ii}^s + \frac{1}{2} Q_{ii}^p \tau_{ii}^p + V_i + \bar{Q}_{ii} \tau_{ii}^s \right) \right], \quad i \in \mathcal{I},$$
 (11j)

$$v_{ij} = v_f \left[1 + 0.15 \left(\frac{Q_{ij}^s + \frac{1}{2} Q_{ij}^p + X_j^+ + \bar{Q}_{ij}}{C_p} \right)^4 \right]^{-1}, \qquad i, j \in \mathcal{I}; \ i \neq j,$$
 (11k)

where A_i denotes the area of zone i and \bar{Q}_{ij} denote the background travel demand.

Eqs. (11j) and (11k) rewrite Eqs. (5a) and (5b) by specifying vehicle density and flow. The vehicle time within zone i consists of four parts: $Q_{ii}^s \tau_{ii}^s$ (contributed by solo rides in zone i), $\frac{1}{2}Q_{ii}^p\tau_{ii}^p$ (contributed by pooling rides in zone i), V_i (contributed by vacant ride-hail vehicles), and $\bar{Q}_{ii}\tau_{ii}^s$ (contributed by background trips). Here, we assume the average travel time of background traffic is identical to that of solo rides. Also, since the analysis period is normalized to a unit time, the total vehicle time divided by zone area A_i yields the vehicle density in the zone. Likewise, the cross-zone vehicle flow from i to j consists of the following: Q_{ij}^s (solo trip flows from i to j), $\frac{1}{2}Q_{ij}^p$ (pooling trip flows from i to j), X_j^+ (relocation trip flow from i to j), and \bar{Q}_{ij} (background trip flow).

Eqs. (11e)–(11g) specify the densities of waiting passengers and vacant vehicles when the matching process is at the stationary state. Specifically, the number of waiting passengers $\Pi_i^s A_i$ ($\Pi_{ij}^p A_i$) equals $\sum_j Q_{ij}^s w_i^s$ ($Q_{ij}^p w_{ij}^p$) as per Little's formula (Little, 1961).

Let $\mathbf{x} = (\mathbf{w}_s, \mathbf{w}_p, \mathbf{v}) \in \mathbb{R}^{12}$. Then, the equation system (11) can be viewed as a fixed-point system $\mathbf{x} = F(\mathbf{x})$. With mild assumptions, we can show a solution to this fixed-point system always exists. The proof would invoke the Brouwer's theorem (Brouwer, 1911), as detailed in Zhang and Nie (2021) for an aggregate market equilibrium model. In brief, two conditions must be satisfied to secure the existence of a fixed point. First, the mapping $F(\cdot)$ must be continuous. This clearly holds as every equation defined in the system (11) is continuous. Second, the map-

ping $F(\cdot)$ must map a compact set to itself. The second condition is reduced to the requirement that every decision variable is bounded. Zhang and Nie (2021) establish the lower and upper bounds on \mathbf{w}_s and \mathbf{w}_p . Their proof of existence can be easily extended to Eq. (11) since the newly added variable \mathbf{v} is naturally bounded between 0 and the free-flow speed v_f .

5 Platform pricing strategy

We proceed to formulate the platform's optimal pricing problem in this section. The platform aims to maximize an objective by choosing trip fares of solo and pooling rides (\mathbf{f}_s and \mathbf{f}_p), as well as the rate of compensation (η) paid to drivers. In what follows, Sections 5.1 and 5.2 consider profit- and welfare-maximization pricing problems, respectively. In Section 5.3, regulations are incorporated into the pricing problem as constraints.

5.1 Profit-maximization

In the absence of regulations, the platform's optimal pricing problem can be formulated as follows:

$$\max_{\mathbf{f}_{s},\mathbf{f}_{p},\eta} R = \frac{1}{\sum_{i} A_{i}} \left[\mathbf{f}_{s}^{T} \mathbf{Q}_{s} + \mathbf{f}_{p}^{T} \mathbf{Q}_{p} - \eta \left(\boldsymbol{\tau}_{s}^{T} \mathbf{Q}_{s} + \frac{1}{2} \boldsymbol{\tau}_{p}^{T} \mathbf{Q}_{p} \right) \right],$$
(12a)

In Eq. (12a), the profit R equals the total revenue $\mathbf{f}_s^T \mathbf{Q}_s + \mathbf{f}_p^T \mathbf{Q}_p$ less the operation $\cos \eta (\boldsymbol{\tau}_s^T \mathbf{Q}_s + \frac{1}{2} \boldsymbol{\tau}_p^T \mathbf{Q}_p)$. For the convenience of presentation, R is normalized by the study area $\sum_i A_i$.

Problem (12) is not easy to analyze because it is an optimization problem defined over a set of highly nonlinear equilibrium constraints. In fact, even finding its numerical solutions is a nontrivial exercise. A challenge unique to the spatial equilibrium model arises from the non-smooth projection operator used to define the relocation flow in Eq. (11c). Left without treatment, such a non-smooth operator may create oscillations in an iterative solution procedure, especially within the neighborhood of $X_i = 0$. To solve this issue, we introduce a SoftPlus function to approximate X_i^+ , i.e.,

$$X_i^+ \simeq \hat{X}_i^+ = \ln\left(1 + e^{X_i}\right).$$
 (13)

It is easy to see that $\hat{X}_i^+ \to 0$ as $X_i \to -\infty$ while $\hat{X}_i^+ \to X_i$ as $X_i \to +\infty$. The evaluation of \hat{X}_i^+ may become numerically unstable when the magnitude of X_i^+ is too large. This problem is resolved by introducing an adjustable scalar γ to scale down X_i^+ whenever necessary, i.e.,

$$\hat{X}_i^+ = \gamma \ln(1 + e^{X_i/\gamma}). \tag{14}$$

In the solution procedure, γ is adjusted according to X_i such that $X_i/\gamma \leq 10$.

Following Zhang and Nie (2021), we apply a sensitivity-analysis-based (SAB) algorithm to solve the optimal pricing problem. The algorithm differentiates the market equilibrium and iteratively applies the gradient to guide the ascending course towards a local optimum. The

gradient
$$\nabla R = \begin{bmatrix} \partial R/\partial \mathbf{f}_s \\ \partial R/\partial \mathbf{f}_p \\ \partial R/\partial \eta \end{bmatrix}$$
 is evaluated by

$$\frac{\partial R}{\partial \mathbf{f}_s} = \frac{1}{\sum_i A_i} \left[\mathbf{Q}_s^T + (\mathbf{f}_s - \eta \boldsymbol{\tau}_s)^T \frac{\partial \mathbf{Q}_s}{\partial \mathbf{f}_s} + \left(\mathbf{f}_p - \frac{\eta}{2} \boldsymbol{\tau}_p \right)^T \frac{\partial \mathbf{Q}_p}{\partial \mathbf{f}_s} \right], \tag{15a}$$

$$\frac{\partial R}{\partial \mathbf{f}_{p}} = \frac{1}{\sum_{i} A_{i}} \left[\mathbf{Q}_{p}^{T} + (\mathbf{f}_{s} - \eta \boldsymbol{\tau}_{s})^{T} \frac{\partial \mathbf{Q}_{s}}{\partial \mathbf{f}_{p}} + \left(\mathbf{f}_{p} - \frac{\eta}{2} \boldsymbol{\tau}_{p} \right)^{T} \frac{\partial \mathbf{Q}_{p}}{\partial \mathbf{f}_{p}} \right], \tag{15b}$$

$$\frac{\partial R}{\partial \eta} = \frac{1}{\sum_{i} A_{i}} \left[(\mathbf{f}_{s} - \eta \boldsymbol{\tau}_{s})^{T} \frac{\partial \mathbf{Q}_{s}}{\partial \eta} + \left(\mathbf{f}_{p} - \frac{\eta}{2} \boldsymbol{\tau}_{p} \right)^{T} \frac{\partial \mathbf{Q}_{p}}{\partial \eta} - \left(\boldsymbol{\tau}_{s}^{T} \mathbf{Q}_{s} + \frac{1}{2} \boldsymbol{\tau}_{p}^{T} \mathbf{Q}_{p} \right) \right]. \tag{15c}$$

The partial derivatives on RHS of Eq. (15) can be further expanded. For instance, the derivatives of \mathbf{Q}_s with respect to \mathbf{f}_s is evaluated as

$$\frac{\partial \mathbf{Q}_{s}}{\partial \mathbf{f}_{s}} = \nabla_{\mathbf{u}_{s}} \mathbf{Q}_{s} \left[I + \nu \left(\frac{\partial \mathbf{w}_{s}}{\partial \mathbf{f}_{s}} + \nabla_{\mathbf{v}} \boldsymbol{\tau}_{s} \frac{\partial \mathbf{v}}{\partial \mathbf{f}_{s}} \right) \right] + \nabla_{\mathbf{u}_{p}} \mathbf{Q}_{s} \left[\nu \left(\frac{\partial \mathbf{w}_{p}}{\partial \mathbf{f}_{s}} + \nabla_{\mathbf{v}} \boldsymbol{\tau}_{p} \frac{\partial \mathbf{v}}{\partial \mathbf{f}_{s}} \right) \right], \tag{16}$$

where $\nabla_{\mathbf{u}_s} \mathbf{Q}_s$ ($\nabla_{\mathbf{u}_p} \mathbf{Q}_s$) represents the gradient of solo demand with respect to utility \mathbf{u}_s (\mathbf{u}_p), $\nabla_{\mathbf{v}} \boldsymbol{\tau}_s$ ($\nabla_{\mathbf{v}} \boldsymbol{\tau}_p$) refers to the gradient of solo (pooling) trip duration with respect to travel speed \mathbf{v} , and I denotes the identity matrix.

Therefore, to derive ∇R , one need to first obtain the derivatives of $\mathbf{x} = (\mathbf{w}_s, \mathbf{w}_p, \mathbf{v}) \in \mathbb{R}^{12}$ with respect to the decision variables $\mathbf{y} = (\mathbf{f}_s, \mathbf{f}_p, \eta) \in \mathbb{R}^9$. This is done by differentiating the fixed-point system:

$$\frac{\partial \mathbf{x}}{\partial \mathbf{y}} = \frac{\partial F(\mathbf{x}, \mathbf{y})}{\partial \mathbf{y}} = \nabla_{\mathbf{x}} F \frac{\partial \mathbf{x}}{\partial \mathbf{y}} + \nabla_{\mathbf{y}} F, \tag{17}$$

where $\nabla_{\mathbf{x}}F$ and $\nabla_{\mathbf{y}}F$ are the partial derivatives of $F(\mathbf{x},\mathbf{y})$ with respect to \mathbf{x} and \mathbf{y} , respectively, and they can be computed using automatic differentiation (Baydin et al., 2017). Accordingly, $\partial \mathbf{x}/\partial \mathbf{y}$ can be solved from the linear system Eq. (17). The readers are referred to Zhang and Nie (2021) for more details.

In this study, we implement Adam (Kingma and Ba, 2014), an adaptive optimization algorithm that makes use of moment information to adaptively scale the "learning rate" for each decision variable. With $\nabla R^{(n)}$ obtained in the nth iteration, the Adam algorithm updates the current solution as follows:

$$m_1^{(n+1)} = \beta_1 m_1^{(n)} + (1 - \beta_1) \nabla R^{(n)},$$
 (18a)

$$m_2^{(n+1)} = \beta_2 m_2^{(n)} + (1 - \beta_2) \left(\nabla R^{(n)} \right)^2,$$
 (18b)

$$\hat{m}_1 = \frac{m_1^{(n+1)}}{1 - \beta_1^n},\tag{18c}$$

$$\hat{m}_2 = \frac{m_2^{(n+1)}}{1 - \beta_2^n},\tag{18d}$$

$$\mathbf{y}^{(n+1)} = \mathbf{y}^{(n)} + \alpha \frac{\hat{m}_1}{\sqrt{\hat{m}_2} + \varepsilon},\tag{18e}$$

where β_1 and β_2 are exponential decay rates for the moment estimates m_1 and m_2 , $(\cdot)^2$ is an element-wise square operator, α is the step size, and ε is a scalar to avoid zero denominator. In

plain English, Adam maintains m_1 and m_2 as exponential moving averages of ∇R and $(\nabla R)^2$, respectively (Eqs. (18a) and (18b)). The two moment estimates are then rescaled (Eqs. (18c) and (18d)) to obtain the next solution (Eq. (18e)). In this study, we set β_1 and β_2 as 0.9 and 0.999, respectively, and $\varepsilon = 10^{-8}$, following the common practice. The step size α , however, is problem specific and has to be set in a trial-and-error fashion to optimize performance. Finally, to avoid being trapped at a "bad" solution, the solution procedure is usually repeated with multiple initial points.

5.2 Welfare-maximization pricing

We define social welfare as

$$W = \frac{1}{\sum_{i} A_{i}} \left(\mathbf{D}_{0}^{T} \mathbf{\bar{u}} + \mathbf{f}_{s}^{T} \mathbf{Q}_{s} + \mathbf{f}_{p}^{T} \mathbf{Q}_{p} - \int_{0}^{N} g^{-1}(n/S_{0}) dn - \nu \mathbf{\bar{Q}}^{T}(\boldsymbol{\tau}_{s} - \boldsymbol{\tau}_{0}) + T \right).$$
(19)

It consists of five parts:

- Passenger surplus $\mathbf{D}_0^T \bar{\mathbf{u}}$, which measures the total expected generalized cost savings gained by switching from transit to ride-hail services. Note that passenger surplus depends on the form of the demand function $q(\cdot)$, and we will specify it later in Section 7.1.
- The platform's revenue $\mathbf{f}_s^T \mathbf{Q}_s + \mathbf{f}_p^T \mathbf{Q}_p$.
- Drivers' opportunity cost $\int_0^N g^{-1}(n/S_0) dn$, where $g^{-1}(\cdot)$ is the inverse of the CDF of drivers' reservation rate. A related metric frequently evaluated in the numerical experiments is driver surplus, which is computed as the total payment to drivers less the opportunity cost, i.e.,

$$\eta\left(\boldsymbol{\tau}_{s}^{T}\mathbf{Q}_{s}+\frac{1}{2}\boldsymbol{\tau}_{p}^{T}\mathbf{Q}_{p}\right)-\int_{0}^{N}g^{-1}(n/S_{0})\mathrm{d}n.$$
(20)

- The additional travel delay due to the operation of ride-hail service $\nu \bar{\mathbf{Q}}^T(\tau_s \tau_0)$. Here, we assume the other travelers in the system share the same value of time as passengers in the ride-hail market. τ_0 is the travel time experienced by private motorists if the ride-hail service is not operated in the city, in which case all ride-hail passengers would choose transit.
- Tax revenue *T*, which, when applicable, is collected under the congestion mitigation policies.

The formulation of the welfare-maximization pricing problem is the same as Problem (12) except its objective function is replaced by Eq. (19). Accordingly, it can be solved using the same gradient ascent algorithm.

5.3 Pricing under regulations

When regulations are imposed on the ride-hail market. The platform's pricing problem becomes a constrained optimization problem. In other words, the platform needs to determine a pricing

strategy that optimizes its objective (e.g., maximizing profit or social welfare), while satisfying the regulatory constraint (e.g., maintaining a certain vehicle utilization rate). Let $h(\cdot) \leq 0$ denote the regulatory constraints, then the problem for a profit-maximizing platform is written as

$$\max_{\mathbf{y}} R(\mathbf{y}), \tag{21a}$$

$$s.t. \quad h(y) \le 0, \tag{21b}$$

where $\mathbf{y} = (\mathbf{f}_s, \mathbf{f}_p, \eta)$ represents the pricing strategy.

Problem (21) can be solved by a dual gradient ascent algorithm as follows:

$$\mathbf{y}^{(l+1)} = \arg\max_{\mathbf{y}} \mathcal{L}(\lambda^{(l)}, \mathbf{y}) = \arg\max_{\mathbf{y}} R(\mathbf{y}) - \lambda^{(l)} h(\mathbf{y}),$$

$$\lambda^{(l+1)} = \max\left(0, \lambda^{(l)} + \rho h(\mathbf{y}^{(l+1)})\right),$$
(22)

$$\lambda^{(l+1)} = \max\left(0, \lambda^{(l)} + \rho h(\mathbf{y}^{(l+1)})\right),\tag{23}$$

where λ represents the Lagrangian multipliers and ρ is a constant penalty parameter. In each iteration, the subproblem Eq. (22) is first solved using the method discussed in Section 5.1. Then, λ is updated using Eq. (23).

Congestion mitigation 6

In this section, we present three congestion mitigation policies and explain how to model their interactions with the platform's operation. The first two policies impose trip-based or cordonbased congestion fees, whereas the third implements a cruising cap (Schaller, 2017a; NYC Taxi and Limousine Commission, 2019).

6.1 Trip-based congestion fee

In order to encourage pooling and transit, major U.S. cities like New York City and Chicago have started to charge a congestion fee on TNC trips starting and/or ending in a designated zone during peak hours. The charge is set higher for solo rides than pooling rides. To simplify the analysis, we assume a congestion fee c is charged on solo rides only and is internalized into the trip fare of each solo ride.⁸ Hence, the generalized cost for a solo ride becomes

$$u_{ij}^{s} = f_{ij}^{s} + \nu(w_{i}^{s} + \tau_{ij}^{s}) + c_{ij}^{s}, \quad i, j \in \mathcal{I},$$
 (24)

where $c_{ij}^s = 0$ if i = 0, j = 0 (i.e., when the trip both starts and ends in the PA zone), otherwise it equals c.

Since the congestion pricing has no impact on drivers' revenue, the expected earning is the same as dictated by Eq. (10). Besides, the tax revenue is $T = \sum_{ij \in \mathcal{I}} c_{ij} Q_{ij}^s$.

⁸Passing such fees to customers is a common practice among TNC platforms, see e.g., https://www.uber.com/ blog/new-york-city/congestion-surcharge/(Accessed: 2020-09-28).

6.2 Cordon-based congestion fee

A commonly used congestion pricing strategy, though rarely implemented in ride-hail, is the cordon-based congestion fee. Under this policy, each vehicle must pay a toll equal to c if (i) it relocates from PA to CBD without carrying any passengers, or (ii) it delivers a solo trip from PA to CBD. For Case (ii), c is passed on to the trip fare. Hence, c_{ij}^s in Eq. (24) becomes c when i=0,j=1 and 0 otherwise. For Case (i), the congestion fee becomes part of drivers' operating cost. Therefore, the expected earning of a driver becomes

$$e = \frac{1}{N_i} \left[\eta \sum_{j \in \mathcal{I}} \left(Q_{ij}^s \tau_{ij}^s + \frac{1}{2} Q_{ij}^p \tau_{ij}^p \right) - c_i^d X_i^+ \right], \quad i \in \mathcal{I},$$
 (25)

where $c_i^d = c$ if i = 1, and 0 otherwise. Accordingly, the tax revenue becomes $T = \sum_{ij \in \mathcal{I}} c_{ij}^s Q_{ij}^s + \sum_{i \in \mathcal{I}} c_i^d X_i^+$.

6.3 Cruising cap

Vacant vehicle cruising is considered an important contributor to the worsening traffic congestion in city centers (e.g., Erhardt et al., 2019; Beojone and Geroliminis, 2021). As mentioned in Section 1, in New York City, the total vacant vehicle hours had grown by 81% from 2013 to 2017, the majority of which is attributed to the operation of TNC vehicles (Schaller, 2017a). In an attempt to curtail further growth, the city proposed a regulation in 2019 that requires any TNC platform to ensure its fleet spend no more than 31% of total operating time without passenger. However, the policy was challenged in the court and later revoked by the state judge (Guse, 2019).

For the purpose of comparison, we implement a version of the cruising cap policy as follows. We first calculate the vehicle utilization rate in CBD as

$$\mu_1 = 1 - \frac{V_1}{V_1 + Q_{11}^s \tau_{11}^p + \frac{1}{2} Q_{11}^p \tau_{11}^p}.$$
 (26)

Let $\underline{\mu}$ be the lower bound on the utilization rate. Thus, the cruising cap is given by $1 - \underline{\mu}$. The regulatory constraint introduced in Section 5.3 is specified as

$$h(\mathbf{y}) = \underline{\mu} - \mu_1(\mathbf{y}) \le 0. \tag{27}$$

7 Case study

We construct a case study using empirical data collected in the City of Chicago. The study area consists of nine communities, as shown in Figure 2. Around 60% of all TNC trips have both pickup and dropoff location inside the area. Specifically, the orange area covers 29 census tracts that form the congestion zone defined in the city's recent congestion pricing policy⁹. That core area also overlaps with much of the city's central business district (CBD). Accordingly, the remaining study area is classified as a PA zone. Based on this construction, the CBD zone has an area of 6.4 square mile (sqmi) and the PA zone's area is about 22.3 sqmi. Appendix B explains

 $^{^9\}mathrm{See}$ https://www.chicago.gov/city/en/depts/bacp/supp_info/city_of_chicago_congestion_pricing.html.

in detail how the parameters used in the case study are estimated using the publicly available TNC, transit and traffic data.

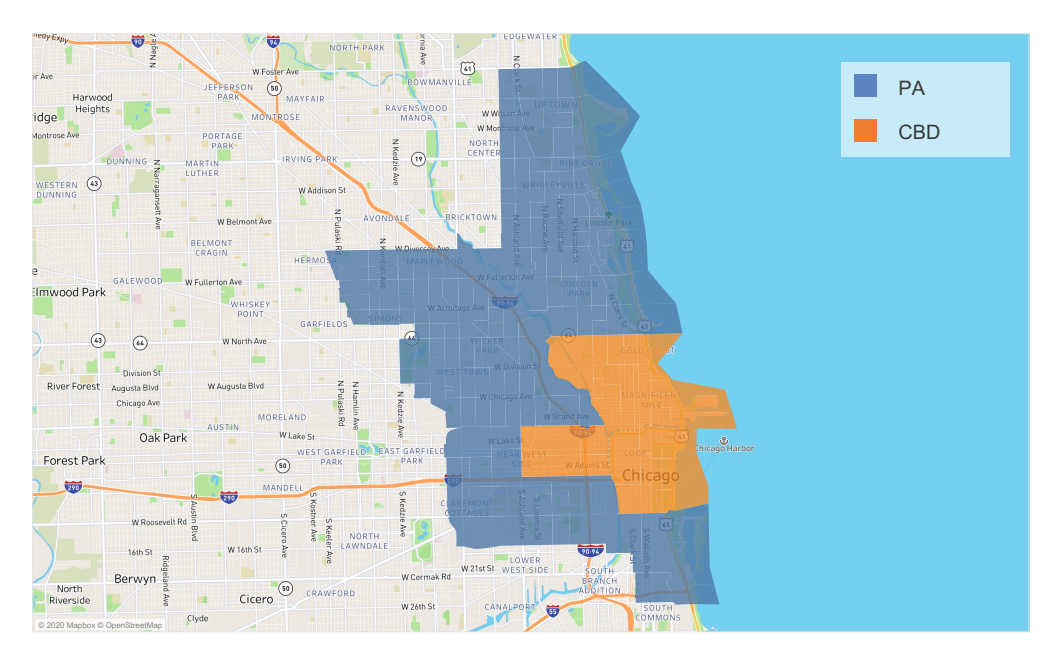


Figure 2: Study area.

In what follows, Section 7.1 first specifies the demand and supply models used in the case study. Section 7.2 analyzes the platform's pricing strategy and the system performance without congestion mitigation policies. Section 7.3 examines and compares the impact of the three policies on the platform's profitability, ride-hail level of service, and social welfare.

7.1 Model specification

We estimate passengers' mode choice using a Multinomial Logit (MNL) model, which specifies Eq. (11a) as

Solo rides:
$$Q_{ij}^s = D_{ij}^0 \frac{\exp(-\theta u_{ij}^s)}{\sum_{m \in \mathcal{M}} \exp(-\theta u_{ij}^m)}, \quad i, j \in \mathcal{I},$$
 (28)

Pooling rides:
$$Q_{ij}^p = D_{ij}^0 \frac{\exp(-\theta u_{ij}^p)}{\sum_{m \in \mathcal{M}} \exp(-\theta u_{ij}^m)}, \quad i, j \in \mathcal{I},$$
 (29)

where the non-negative parameter θ measures the uncertainty in the decision-making process. Here, we implicitly assume solo and pooling as two distinct travel modes¹⁰.

With the MNL model, the expected generalized cost saving $\bar{\mathbf{u}}$ (see Eq. (19)) can be quantified using the well-known logsum term (also known as the accessibility measure). Specifically, each

¹⁰These two modes may be similar enough to justify the use of a nested multinomial logit model. However, properly estimating a nested model from empirical data is beyond the scope of the present study. Zhang and Nie (2021a) compare a nested logit model with an MNL in a very similar setting and conclude the use of a nested model has limited impact on the main results of their study, although it reduces the total market share of ride-hail.

element in $\bar{\mathbf{u}}$ is given by

$$\bar{u}_{ij} = \frac{1}{\theta} \log \sum_{m \in \mathcal{M}} \exp[\theta(u_{ij}^t - u_{ij}^m)], \quad i, j \in \mathcal{I}.$$
(30)

For simplicity, we assume each driver's reservation rate \tilde{e}_0 follow a uniform distribution over a range $[\underline{e}_0, \overline{e}_0]$. Accordingly, Eq. (11b) can be rewritten as

$$(\bar{e}_0 - \underline{e}_0)N^2 + \underline{e}_0 S_0 N - e S_0 = 0, \tag{31}$$

from which $N = \sum_{i \in \mathcal{I}} N_i$ can be easily solved as the positive root. Finally, the driver's opportunity cost defined in Eq. (19) is reduced to

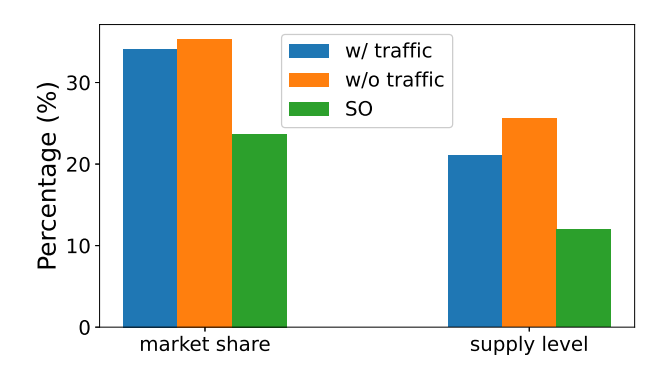
$$\int_0^N G^{-1}(n/S_0) dn = \frac{\bar{e}_0 - \underline{e}_0}{2S_0} N^2 + \underline{e}_0 N.$$
(32)

7.2 Unregulated market

We first compare the system performance under profit- and welfare-maximization pricing in an unregulated market. For simplicity, they are referred to as monopoly (MO) and social optimum (SO) pricing, respectively. For MO pricing, we consider another case where the platform fails to anticipate the impact of its operation on traffic congestion. That is, it optimizes the pricing policy based on a default, flow-independent speed. However, the actual effect of this "sub-optimal" pricing policy will be evaluated according to a market equilibrium that does characterize traffic congestion. We are particularly interested in the following question: *should the platform "care" about traffic congestion even if it is completely motivated by self-interest (i.e., profit)?*

Figure 3 illustrates the overall ride-hail market share and supply level in the three studied scenarios: "w/ traffic" as MO pricing considering traffic congestion, "w/o traffic" as MO pricing without considering traffic congestion, and "SO" as SO pricing considering traffic congestion. The market share is defined as the percentage of the potential passengers $(\sum_{i,j\in\mathcal{I}}D^0_{ij})$ who opt for ride-hail service, whereas the supply level is the percentage of potential drivers (S_0) who join the workforce of the platform. As expected, when traffic congestion is ignored, the platform tends to hire more drivers and serves more trips. In contrast, at system optimum, the ride-hail market is much smaller in both demand and supply. The drop in vehicle supply is especially steep: almost half of the drivers would leave the market under an SO pricing regime.

Figure 4 plots the ride-hail market share by OD pair and mode. First, under no circumstance is pooling observed in the peripheral trips. Pooling within the PA zone is unattractive because the demand is low and scattered. The former leads to long pickup detour, while the latter results in long en-route detour. Second, the share is the lowest for central trips, due to a much more competitive transit service in this area. This is especially true under SO pricing. In this case, almost no central trips are served by ride-hail vehicles. Evidently, given the quality of transit services available in Chicago downtown, the net utility generated by switching from transit to ride-hail is barely enough to offset the negative traffic impact. Interestingly, when the platform ignores the congestion effect, it also stops serving pooling trip inside CBD. This decision is rendered likely because (i) the solo trips are more profitable and (ii) the platform underestimate the traffic impact of forgoing pooling trips all together. Third, for inter-zonal markets, ride-hail



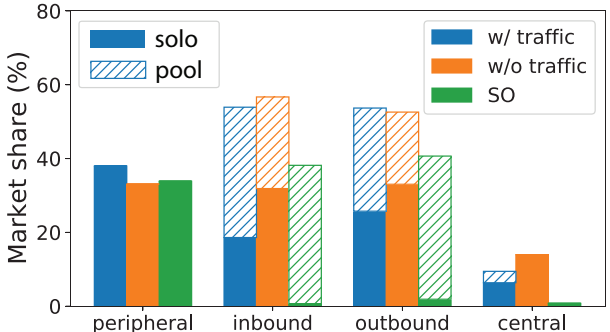


Figure 3: Market share and supply level.

Figure 4: Share by market segments.

performs much better, in some case capturing well over 50% of the market share. Moreover, the majority of inbound trips are pooled when the congestion effect is taken into account. On the other hand, the pooling ratio is lower under MO pricing without considering traffic, especially for trips originated in CBD. Since solo rides require more vehicle time, failing to anticipate the traffic impact is likely to inadvertently worsen traffic congestion in CBD. Finally, the SO pricing strongly encourages pooling. In fact, in both inter-zonal market segments, nearly all trips are pooled.

Figure 5 reports the four components of social welfare under the three pricing policies. As expected, MO pricing with traffic delivers the highest profit to the platform, while the profit generated by SO pricing is the lowest. Drivers benefit the most from MO pricing without traffic, because the platform tends to hire more drivers in this case. On the contrary, passengers are slightly better off when the congestion effect is accounted for. SO pricing, on the other hand, minimizes the traffic impact of ride-hail at the expense of other stakeholders. The biggest losers are the drivers, whose surplus is reduced to but a fraction of what they would receive under MO pricing.

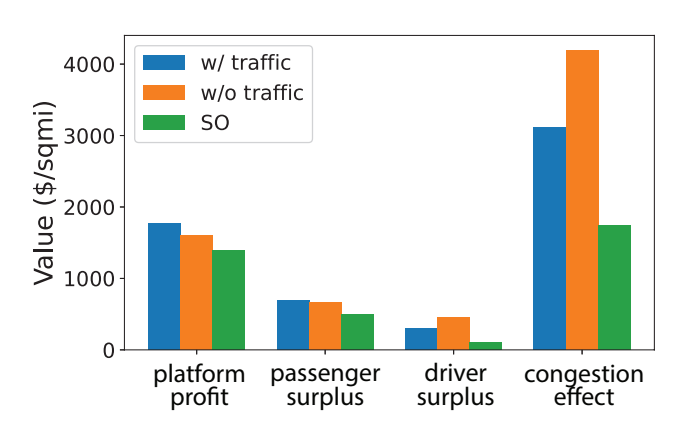


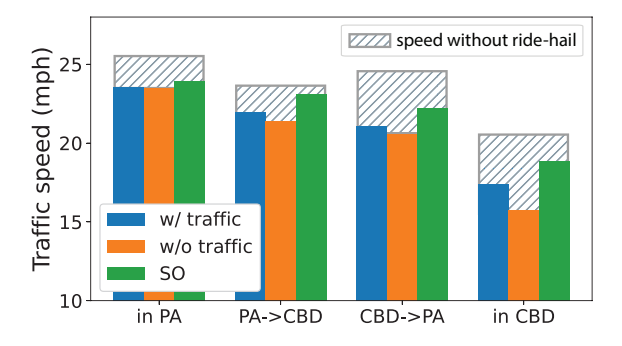
Figure 5: Components of social welfare.

As illustrated in Figure 5, in all scenarios, traffic congestion plays a major role in shaping social welfare: its value is comparable to that of the other three combined in all three cases. In particular, for MO pricing without traffic, the sum of net benefits gained by the platform, passengers and drivers is not nearly enough to make up for the loss due to worsened congestion. Figure 6 compares travel speed in the three scenarios. It shows the operation of ride-hail service lowers the travel speed by up to 5 mph. Although the overall speed reduction seems modest, the cumulative effect is

nonetheless considerable because of the sheer size of background traffic ($\bar{\mathbf{Q}}$ in Eq. (19)). Figure 6 also indicates that the largest reduction occurs inside CBD, which agrees with recent empirical findings (Erhardt et al., 2019; Diao et al., 2021). Compared to MO pricing, SO pricing has

the most modest impact on traffic speed, hence a significantly smaller congestion cost in social welfare (see Figure 5).

Figure 7 plots both occupied and vacant VMT inside each zone and between zones. It suggests that a significant amount of vacant VMT exist in both CBD and PA. This is expected, as a certain amount of vacant vehicles is needed in each zone to maintain a reasonable LOS. On the other hand, the vacant VMT between zones is due to vehicle relocation. It is interesting to see that relocation trips are only observed in the case of MO pricing without traffic. This phenomenon indicates that the pricing policy fails to balance the demand and supply across zones. Specifically, by overlooking congestion, the platform attracts more drivers into CBD than what the demand in the zone could adequately consume. Consequently, at equilibrium, some drivers would relocate to PA, suffering a dead-weight loss in the process. This problem is rooted in the sub-optimal nature of MO pricing without traffic.



occupied w/ traffic w/o traffic so so so in PA PA->CBD CBD->PA in CBD

Figure 6: Travel speed inside and between zones.

Figure 7: Ride-hail vehicle miles traveled (VMT) inside and between zones.

Note that, in Figure 7, the occupied VMT inside CBD and PA only accounts for the intra-zonal trips. Hence, when computing the vehicle occupancy rate associated with each zone market, one need to include the occupied VMT of inter-zonal trips as well. Consequently, the occupancy rate in the CBD zone is greater than the PA zone, though this is not clearly illustrated in the figure. Overall, SO pricing produces the lowest total vacant VMT whereas MO pricing without traffic leads to the highest. The difference is more significant in CBD. As shown in Figure 4, a profit-maximization platform (i.e., MO pricing) tends to serve more trips originated from CBD. It thus requires more vacant vehicle time inside CBD to support a desired LOS.

7.3 Regulated market

In this section, we investigate the impact of the three congestion mitigation policies discussed in Section 6. For both trip-based and cordon-based policies, the congestion fee varies from \$0.2 to \$2. The cruising cap ranges between 0.3 and 0.6, which is equivalent to a minimum occupancy between 0.4 and 0.7. The results without regulations are also included to benchmark the performance of tested policies. Specifically, the result of MO pricing with traffic represents the status quo, while that of SO pricing represents the "desirable outcome".

7.3.1 Market share

Figure 8 shows the total market share of ride-hail service rises under the two congestion pricing policies, though the growth is rather mild (less than 2%). With the cruising cap, the market share first increases in parallel with the congestion pricing policies, but begins to drop precipitately when the minimum occupancy exceeds 0.5. However, it remains well above the level achieved by SO pricing, even when a minimum occupancy of 0.7 is imposed.

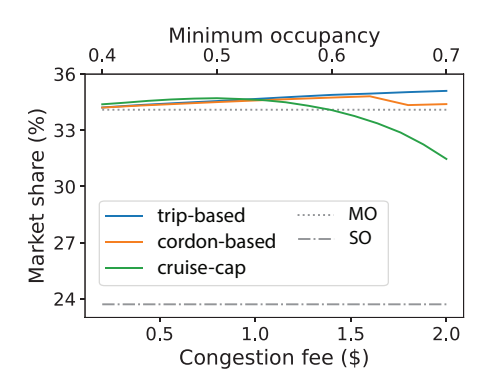


Figure 8: Ride-hail market share

While the total market share is relatively stable, the shares between different OD pairs vary a lot with service mode and congestion mitigation policies, as reported in Figure 9. The share of the peripheral trips hardly changes because these trips are not hit by any of the policies. For all other three OD pairs, a large portion of solo rides is replaced by pooling rides under the trip-based policy. The cordon-based policy, however, only produces a similar effect on inbound trips as its trip-based counterpart. It does cause around 5% of outbound trips to switch from solo to other modes, primarily transit, but has almost no impact at all on central trips. These findings are expected, because the trip-based congestion fee

targets solo passengers who travel to, from and in CBD whereas the cordon-based fee only affects inbound travelers. However, when the congestion fee increases beyond \$1.6/veh, the platform only serves solo trips inside CBD, which causes a sudden drop in the share of pooling trips to zero (see the last panel in Figure 9(b)). The performance of the cruising cap is peculiar. The regulation forces the platform to sacrifice its market share in the inter-zonal trips in exchange for an uptick in both solo and pooling rides in CBD. This is not a desired outcome because the extra trips it attracts could have used a descent transit service.

7.3.2 Level of service and congestion relief

Figures 10 and 11 plot passenger wait time and vacant vehicle density in PA and CBD, respectively. The wait time is an average weighted by demand for each mode and OD pair. The most intriguing finding here is that passengers have to endure a much longer wait time when a cruising cap is imposed. Those traveling from CBD see their wait times jump from around six minutes to well above 10 minutes as the minimum occupancy grows from 0.4 to 0.7. The increase in wait time is accompanied by a decline in vacant vehicle density, which is steeper as the cap becomes more restrictive (see Figure 11).

Interestingly, the average wait time remains almost intact under both congestion pricing policies. The vacant vehicle density, however, had a more noticeable dip, especially in CBD. At first glance, this result is somewhat puzzling, because one would expect a lower vacant vehicle density to prolong waiting. It also appears to contradict with Li et al. (2020), who find trip-based fee hurts the LOS in the peripheral area. We believe the discrepancy can be explained by the availability of pooling in our model. As revealed in Figure 9, more inbound passengers end up choosing to pool, which helps maintain a sufficient vehicle supply in PA. On the other hand, the demand for ride-hail service, particularly solo trips, is depressed in CBD. Hence, the passenger

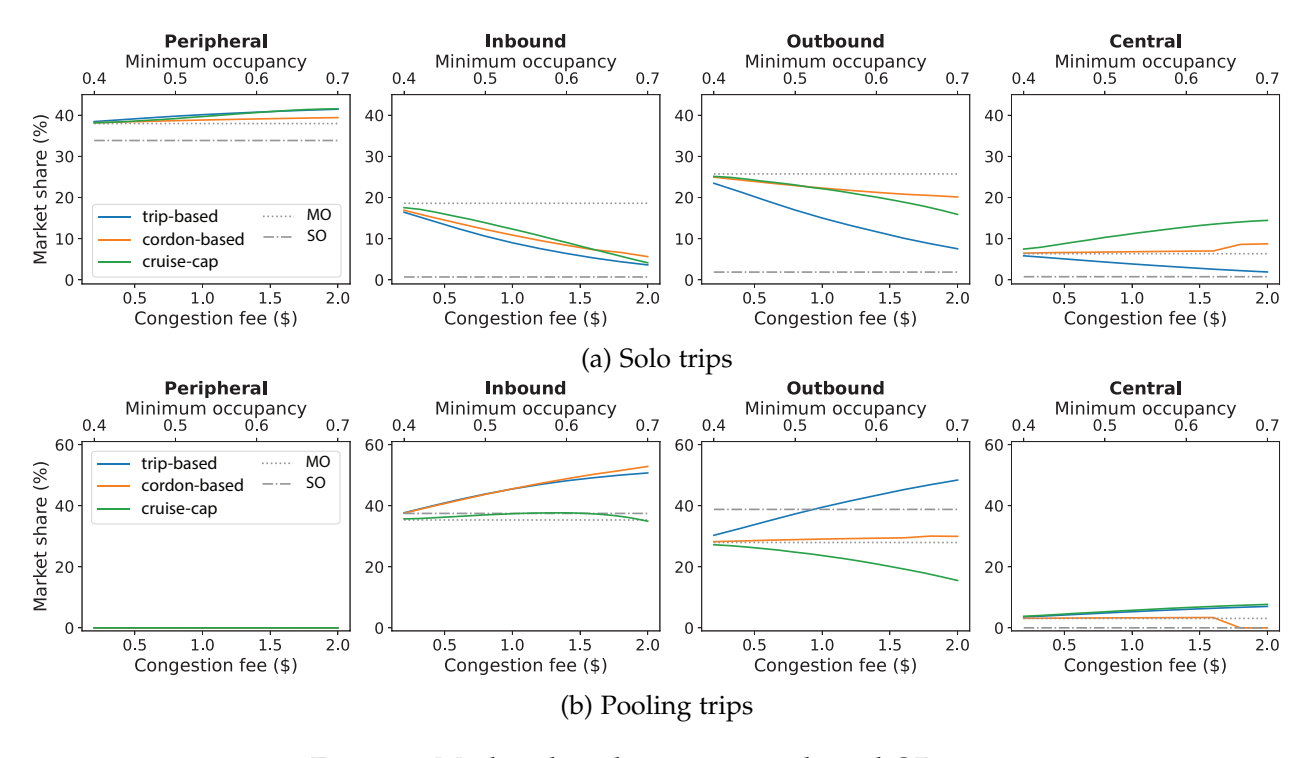


Figure 9: Market share by service mode and OD pair.

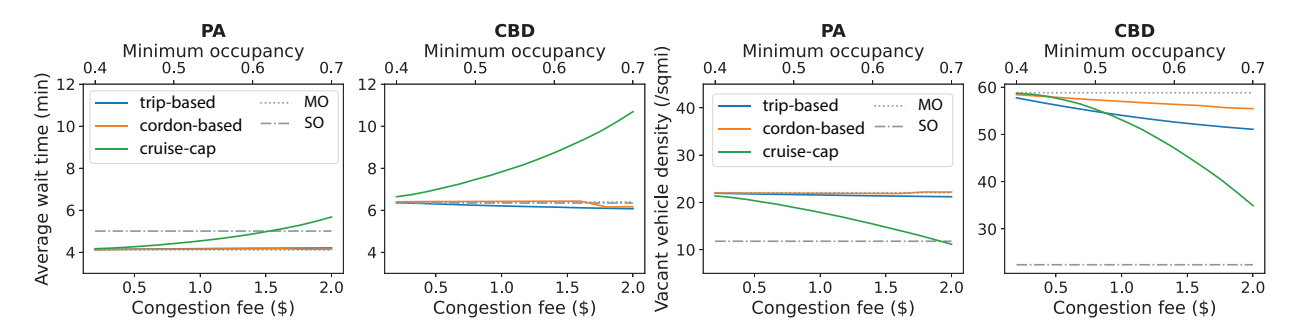


Figure 10: Passenger wait time by zone.

Figure 11: Vacant vehicle density by zone.

wait time is hardly affected even though the vacant vehicle density drops.

Another observation from Figure 11 is how little the two congestion pricing policies had done to move vacant vehicle density towards the SO level. This is true in both PA and CBD, although the gap is much larger in the latter. Thus, these policies may not be effective instruments to reduce vacant vehicle cruising. As suggested in Figures 12 and 13, their contribution to traffic relief is also minor. Under both trip- and cordon-based pricing policies, the improvement in travel speed across all market segments is barely visible. Similarly, vacant VMT were little affected, though occupied VMT were reduced much more thanks to the greater reliance on pooling. As for the cruising cap, it achieves vacant VMT at the SO level when the minimum occupancy requirement reaches 0.7. Yet, the occupied VMT is still far away from that at SO. Furthermore, the reduced vacant VMT only helps improve the inter-zonal travel speed. As shown in Figures 12, the congestion in CBD becomes even worse.

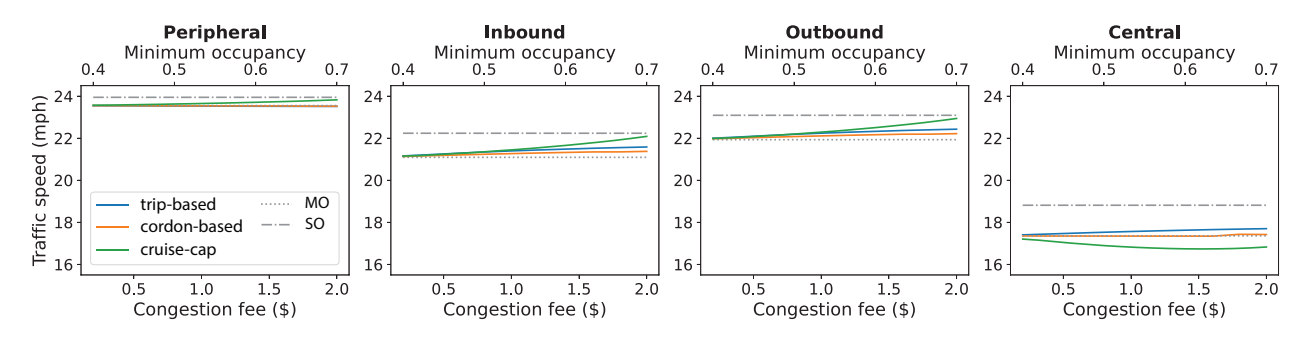


Figure 12: Travel speed by OD pair.

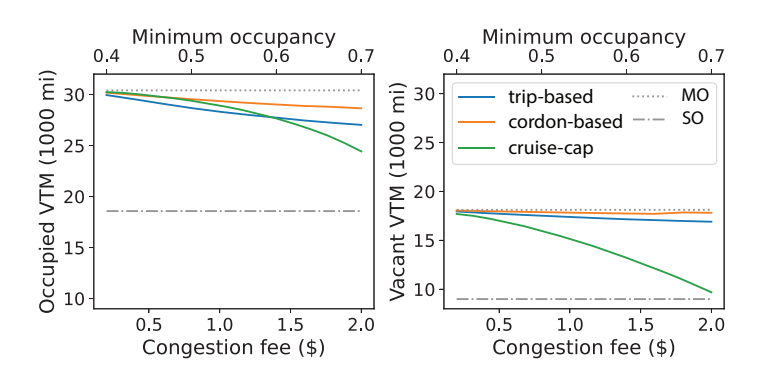


Figure 13: VMT by vehicle status.

7.3.3 Fare and compensation

Figure 14 reveals how the platform's pricing strategy varies with the congestion mitigation policies ¹¹. We can see that the fares under the two congestion pricing policies are quite similar to those under MO pricing. Hence, the shift in demand is largely caused by the congestion fee directly charged on passengers. In contrast, to meet the cruising cap requirement, the platform has to more actively manipulate the price. Notably, it aggressively lowers the price for both solo and pooling trips in CBD to make them so much more attractive that the occupancy rate could be sustained at the required level. Meanwhile, it increases the fare for inbound trips—especially the solo ones—and reduces that for outbound trips. This maneuver is meant to discourage inbound travel and encourage outbound travel. Intuitively, moving vehicles out of CBD on occupied trips could help reduce vehicle cruising in CBD and thus release the pressure of cruising cap. However, this strategy does not attract more demand (see Figure 9), due primarily to the deteriorating LOS (see Figure 10).

Figures 15 and 16 plot the compensation rate paid to drivers and the vehicle supply associated with each zone, respectively. It is clear that drivers are paid much less at SO, which results in a smaller vehicle supply in the market. While the compensation rate is reduced slightly by the two congestion pricing policies, it is still much higher than the SO level. Under the cruising cap, however, the compensation rate plunges. Despite this suffering, the cruising cap does not effectively control vehicle supply in CBD except when the cap is highly restrictive. A mild cap

¹¹The pooling trip fare for peripheral trips is not plot because no trip is pooled. The same applies to central trips with cordon-based fee beyond \$1.6/veh.

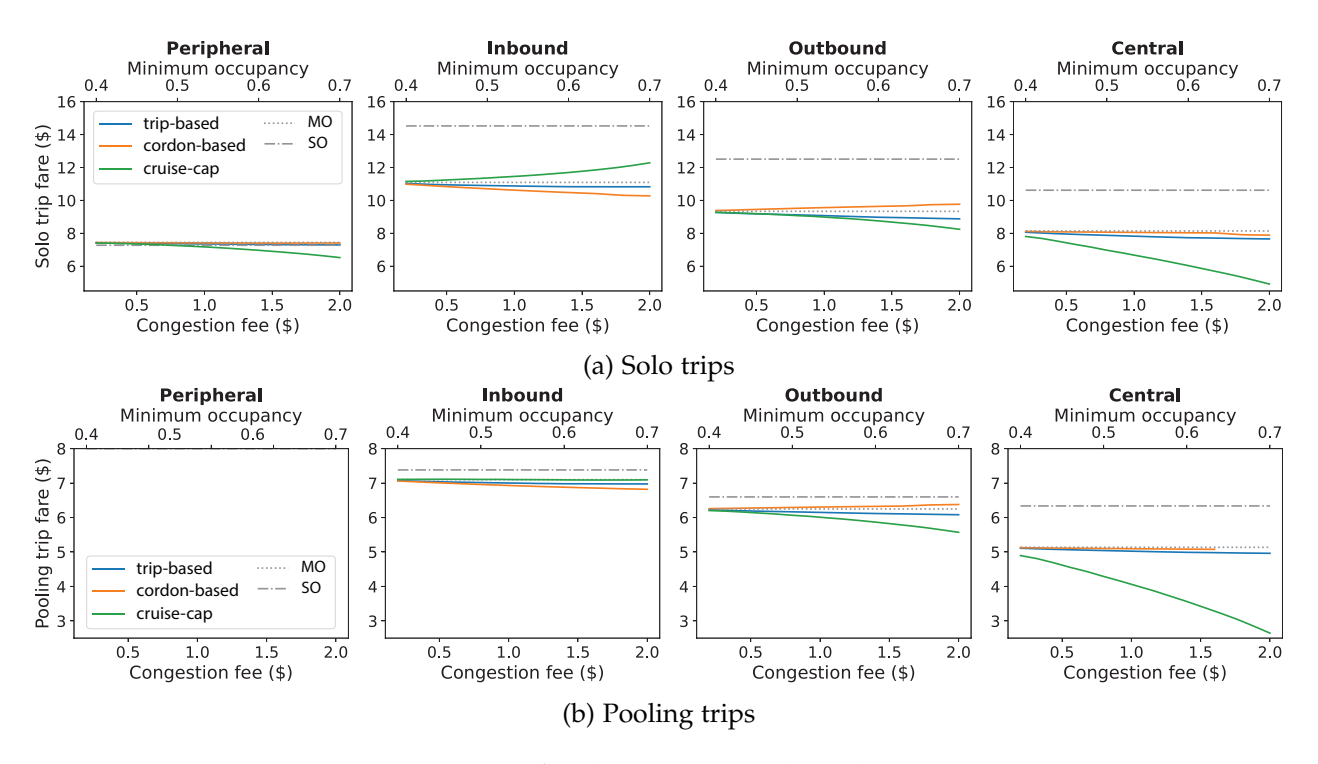


Figure 14: Trip fare by service mode and OD pair.

actually induces more vehicles to enter CBD because the platform seeks to serve more trips there under the circumstance (see Figure 9). In contrast, under SO pricing, almost all trips inside CBD are served by transit. As indicated in Figure 14, such an outcome requires the platform to raise price on both solo and pooling rides, while cutting the compensation to drivers. However, none of the three mitigation policies could achieve such an outcome, not even close.

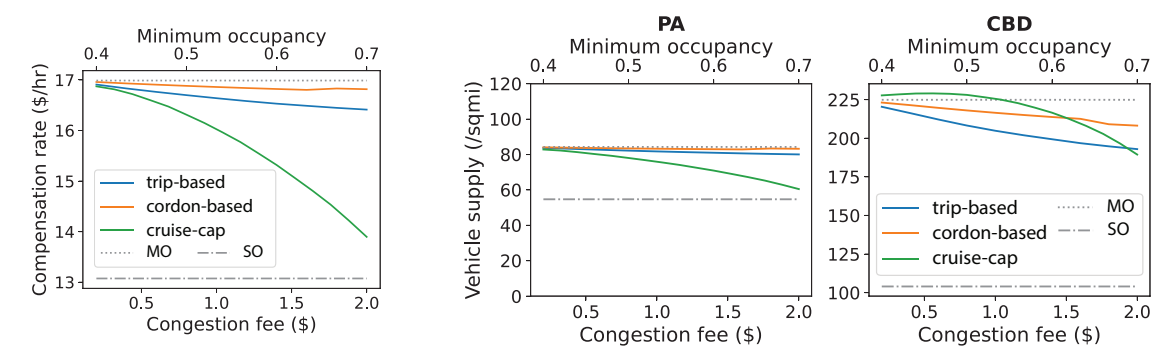


Figure 15: Compensation rate.

Figure 16: Vehicle supply by zone.

7.3.4 Discussions

In this section, we further discuss the performance of the three tested policies by comparing their welfare effects. As seen in Figure 17(a), both trip- and cordon-based pricing policies yield a net gain in social welfare, whereas the cruising cap leads to a net loss. Although the trip-based fee stands out as a clear winner, its overall welfare outcome still falls far behind that under SO

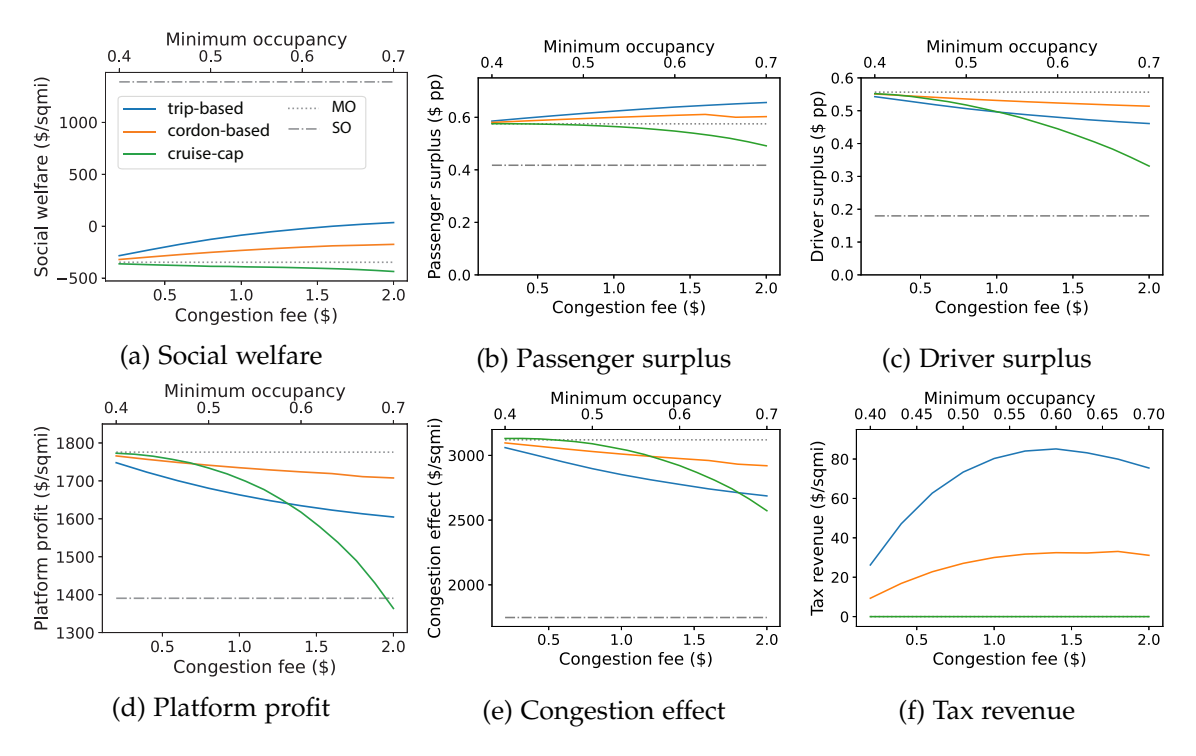


Figure 17: Social welfare by part.

pricing.

A closer look at different welfare components reveals that the two congestion pricing policies give ride-hail passengers a modest benefit at the expense of drivers and the platform (see Figures 17(b)-(d)). The cruising cap, however, hurts all three stakeholders. With the most restrictive cap, the driver surplus decreases almost 40% and the platform loses over 20% of its profit. Indeed, in this case the platform earns even less than under SO pricing.

At 2\$/ride, the trip-based fee realizes about a one-third of the reduction in the congestion cost achieved by SO pricing, more than doubling the improvement obtained by the cordon-based fee (see Figure 17(e)). This finding seems surprising at first glance given the small improvement in travel speed (see Figure 12). Yet, it is important to note that the traffic generated by TNC rides is a rather small fraction of the total vehicular traffic (around 5%). Hence, whatever gains in travel speed would be magnified by a large number of background trips. Indeed, even the SO pricing can only increase the average speed by 2 mph. Despite its seemingly more dramatic impact on vacant VMT and travel speed, the cruising cap policy did not bring about an overwhelming congestion relief. Even at the extreme (minimum occupancy = 0.7), its congestion savings is still well below 50% of what is obtained by SO pricing. With milder restrictions on vehicle occupancy rate (below 0.56), the cruising cap actually trails behind both congestion pricing policies. This seemingly counter-intuitive result is likely due to the negative impact of cruising cap on travel speed in CBD (see Figure 12). Since most trips are concentrated in the city center, each unit of decrease in average speed in CBD inflicts a large external cost. Accordingly, the extra cost induced by the more intense congestion in CBD offsets the savings from PA and inter-zonal trips.

Finally, the trip-based policy is good at generating tax revenues. At every congestion fee tested, it collects more than twice as much revenue as the cordon-based policy does (see Figure

17(f)). This finding is also expected as trips between more OD pairs are charged under trip-based pricing compared to cordon-based policy. For the trip-based policy, the tax revenue is maximized at around \$1.4/trip, while that for the cordon-based policy is around \$1.8/veh.

To summarize, trip-based pricing seems to be the best of the three regulations considered herein. It improves social welfare, benefits passengers, reduces the congestion cost and generates a substantial amount of tax revenues. Curiously, drivers and the platform are always losers, regardless of which congestion mitigation policies is adopted. Their losses are the smallest under cordon-based pricing. On the other hand, the cruising cap policy delivers the worst outcomes. Even though it improves traffic speed outside CBD, the policy does not benefit any stakeholder or generate any tax revenue. Furthermore, the cruising cap hits drivers and the platform much harder than the other two, especially when a highly restrictive cap is implemented. As a result, the system is worse off in terms of social welfare, compared to the unregulated benchmark.

8 Conclusions

We analyzed the impact of three congestion mitigation policies on an idealized urban transportation system represented by a two-node spatial market equilibrium model. In the system, a transportation network company (TNC) offers both solo and pooling services to passengers who also have transit as a fallback option. The market equilibrium model is built on two sub-models: an aggregate congestion model describing the traffic impact of TNC vehicles on all travelers in the system, and a matching model estimating the TNC's level of service based on the interactions between passengers and TNC drivers. Based on the equilibrium model, we formulate and propose solution algorithms to the platform's optimal pricing problems, in which the TNC seeks to optimize profits or social welfare subject to the extra costs and/or constraints imposed by the congestion mitigation policies.

The main findings from our case study, constructed using empirical data from Chicago, are summarized as follows.

- TNC operations have a considerable impact on traffic congestion, even though they contribute only 5% to the total traffic. Failing to anticipate congestion in the optimal pricing problem leads to sub-optimal decisions that not only worsen traffic congestion by inducing extra supply, but also hurt the TNC's profitability.
- Welfare-maximization pricing strongly encourages pooling in all but peripheral trips. In
 the city center, it raises the price on both solo and pooling rides in favor of transit. This is
 because the net utility generated by switching from transit to TNC in the city center, where
 the transit service has a high LOS, is hardly enough to offset the negative traffic impact.
 In contrast, profit-maximization pricing tends to serve more central trips with less pooling.
 To do so, more vehicles must be induced to the city center, which exacerbates overall traffic
 conditions.
- The trip- and cordon-based congestion mitigation policies modestly reduce the extra congestion cost caused by unregulated TNC operations, even though the positive impact on average travel speeds is barely discernible. They both promote pooling, which help cut the

occupied vehicle miles traveled. While the cruising cap imposed in the city center substantially brings down the total vacant vehicle miles traveled, it does not offer an overwhelming congestion relief. Paradoxically, the policy could worsen traffic conditions in the city center, where most trips originate, as it pushes the platform to serve more trips there.

• Of the three policies considered herein, the trip-based policy delivers the best overall performance. It lifts the system's social welfare while keeping the TNC's level of service almost intact. While it does slightly disadvantage the TNC and its drivers, the benefits it creates for travelers, in the form of congestion relief, consumer surplus and tax revenue, more than make up for this loss. The cordon-based policy demonstrates similar behaviors as the trip-based policy, but trails behind in nearly all metrics. The cruising cap policy is a surprising disappointment. While the private motorists benefit from the extra congestion relief the policy promises to deliver, the other stakeholders together suffer a much greater loss.

In this study, we simplify the urban transportation system as a two-node model since most congestion mitigation policies in practice target TNC operations in the central business district of a city. By adopting a static view of the market equilibrium, we also ignore the time-of-day variations in all state and decision variables. Hence, the next step is to allow a more general network model that can accommodate policies with higher spatial and temporal resolutions. Such an extension would complicate the modeling of vehicle relocation behaviors, whether they are driven by drivers' self-interest or coordinated by the TNC. Another limitation of the current model is the relatively simplistic treatment of choice behaviors. A future study could consider heterogeneity on the demand side, such as the willingness to share, as well as the interdependence between solo and pooling in mode choice.

Another future direction is to compare the trip-based pricing policy against other policies, such as the fleet size cap policy, or time-based pricing mentioned in Schaller (2018b) and Li et al. (2021), or study the problem of designing "optimal" mitigation policies. An optimal mitigation policy may be trip-based, but with a more flexible structure that allows the congestion charge to vary spatially and/or temporally.

Acknowledgment

The research was supported by the US National Science Foundation under the award number CMMI 1922665.

References

- M. J. Alonso-González, O. Cats, N. van Oort, S. Hoogendoorn-Lanser, and S. Hoogendoorn. What are the determinants of the willingness to share rides in pooled on-demand services? *Transportation*, 48(4):1733–1765, 2021.
- J. D. Angrist, S. Caldwell, and J. V. Hall. Uber vs. taxi: A driver's eye view. Technical report, National Bureau of Economic Research, 2017.
- R. Arnott. Taxi travel should be subsidized. Journal of Urban Economics, 40(3):316–333, 1996.

- A. Asadpour, I. Lobel, and G. van Ryzin. Minimum earnings regulation and the stability of marketplaces. Available at SSRN 3502607 (Accessed: 2020-10-25), 2019.
- S. Banerjee, C. Riquelme, and R. Johari. Pricing in ride-share platforms: A queueing-theoretic approach. Available at: SSRN 2568258 (Accessed: 2018-11-12), 2015.
- A. G. Baydin, B. A. Pearlmutter, A. A. Radul, and J. M. Siskind. Automatic differentiation in machine learning: a survey. *The Journal of Machine Learning Research*, 18(1):5595–5637, 2017.
- C. V. Beojone and N. Geroliminis. On the inefficiency of ride-sourcing services towards urban congestion. *Transportation Research Part C: Emerging Technologies*, 124:102890, 2021.
- K. Bimpikis, O. Candogan, and D. Saban. Spatial pricing in ride-sharing networks. *Operations Research*, 2019.
- F. P. Boscoe, K. A. Henry, and M. S. Zdeb. A nationwide comparison of driving distance versus straight-line distance to hospitals. *The Professional Geographer*, 64(2):188–196, 2012.
- A. Braverman, J. G. Dai, X. Liu, and L. Ying. Empty-car routing in ridesharing systems. *Operations Research*, 2019.
- L. E. J. Brouwer. Über abbildung von mannigfaltigkeiten. *Mathematische Annalen*, 71(1):97–115, 1911.
- N. Buchholz. Spatial equilibrium, search frictions and efficient regulation in the taxi industry. Available at https://scholar.princeton.edu/sites/default/files/nbuchholz/files/taxi_draft.pdf (Accessed: 2020-03-04), 2019.
- G. P. Cachon, K. M. Daniels, and R. Lobel. The role of surge pricing on a service platform with self-scheduling capacity. *Manufacturing & Service Operations Management*, 19(3):368–384, 2017.
- J. Castillo, D. T. Knoepfle, and E. G. Weyl. Surge pricing solves the wild goose chase. Available at SSRN 2890666 (Accessed: 2018-5-3), 2018.
- M. K. Chen and M. Sheldon. Dynamic pricing in a labor market: Surge pricing and flexible work on the Uber platform. In *Ec*, page 455, 2016.
- R. R. Clewlow and G. S. Mishra. Disruptive transportation: The adoption, utilization, and impacts of ride-hailing in the united states. Technical report, 2017.
- CNN Business. Prop 22 passes in California, exempting Uber and Lyft from classifying drivers as employees, 2020. URL https://www.cnn.com/2020/11/04/tech/california-proposition-22/index.html.
- J. Cramer and A. B. Krueger. Disruptive change in the taxi business: The case of uber. *American Economic Review*, 106(5):177–82, 2016.
- A. de Palma and R. Lindsey. Traffic congestion pricing methodologies and technologies. *Transportation Research Part C: Emerging Technologies*, 19(6):1377–1399, 2011.

- A. De Palma, M. Kilani, and R. Lindsey. Congestion pricing on a road network: A study using the dynamic equilibrium simulator metropolis. *Transportation Research Part A: Policy and Practice*, 39(7-9):588–611, 2005.
- M. Diao, H. Kong, and J. Zhao. Impacts of transportation network companies on urban mobility. *Nature Sustainability*, pages 1–7, 2021.
- G. W. Douglas. Price regulation and optimal service standards: The taxicab industry. *Journal of Transport Economics and Policy*, pages 116–127, 1972.
- G. D. Erhardt, S. Roy, D. Cooper, B. Sana, M. Chen, and J. Castiglione. Do transportation network companies decrease or increase congestion? *Science advances*, 5(5):eaau2670, 2019.
- G. R. Frechette, A. Lizzeri, and T. Salz. Frictions in a competitive, regulated market: Evidence from taxis. *American Economic Review*, 109(8):2954–92, 2019.
- A. Goodchild, D. Mackenzie, A. Ranjbari, J. Machado, and G. D. Chiara. Curb allocation change project, 2019.
- G. Goodin, R. T. Baker, L. Taylor, et al. Mileage-based user fees: Defining a path toward implementation; phase 2: An assessment of institutional issues. Technical report, Texas Transportation Institute, 2009.
- B. Greenshields, J. Bibbins, W. Channing, and H. Miller. A study of traffic capacity. In *Highway research board proceedings*, volume 1935. National Research Council (USA), Highway Research Board, 1935.
- I. Gurvich, M. Lariviere, and A. Moreno. Operations in the on-demand economy: Staffing services with self-scheduling capacity. In *Sharing Economy*, pages 249–278. Springer, 2019.
- C. Guse. Judge throws out NYC's strict regulations on Uber and Lyft, calls them 'arbitrary', 2019. Available at https://www.nydailynews.com/new-york/ny-judge-lawsuit-uber-lyft-cruising-cap-20191223-q4f4g3xat5gdlkdtm5zlezbtbe-story.html (Accessed: 2020-01-04.
- A. Henao. *Impacts of Ridesourcing-Lyft and Uber-on Transportation Including VMT, Mode Replacement, Parking, and Travel Behavior*. Thesis, University of Colorado at Denver, 2017.
- H. Ho, S. C. Wong, H. Yang, and B. P. Loo. Cordon-based congestion pricing in a continuum traffic equilibrium system. *Transportation Research Part A: Policy and Practice*, 39(7-9):813–834, 2005.
- INRIX Research. Global traffic scorecard. Technical report, 2019.
- J. Ke, H. Yang, X. Li, H. Wang, and J. Ye. Pricing and equilibrium in on-demand ride-pooling markets. *Transportation Research Part B: Methodological*, 139:411–431, 2020a.
- J. Ke, H. Yang, and Z. Zheng. On ride-pooling and traffic congestion. *Transportation Research Part B: Methodological*, 142:213–231, 2020b.

- J. Ke, Z. Zheng, H. Yang, and J. Ye. Data-driven analysis on matching probability, routing distance and detour distance in ride-pooling services. *Transportation Research Part C: Emerging Technologies*, 124:102922, 2021.
- D. P. Kingma and J. Ba. Adam: A method for stochastic optimization. Available at arXiv:1412.6980 (Accessed: 2020-10-26), 2014.
- P. S. Lavieri and C. R. Bhat. Modeling individuals' willingness to share trips with strangers in an autonomous vehicle future. *Transportation research part A: policy and practice*, 124:242–261, 2019.
- S. Li, H. Tavafoghi, K. Poolla, and P. Varaiya. Regulating tncs: Should uber and lyft set their own rules? *Transportation Research Part B: Methodological*, 129, 2019.
- S. Li, H. Yang, K. Poolla, and P. Varaiya. Sptial pricing in ride-sourcing markets under a congestion charge. Available at arXiv:2010.09260 (Accessed 2020-10-26), 2020.
- S. Li, K. Poolla, and P. Varaiya. Impact of congestion charge and minimum wage on tncs: A case study for san francisco. *Transportation Research Part A: Policy and Practice*, 148:237–261, 2021.
- J. D. Little. A proof for the queuing formula: $L = \lambda$ w. Operations research, 9(3):383–387, 1961.
- X. Liu, L. Xu, S. Qian, and W. Ma. A data-driven approach to manage the curbside ride-hailing pick-ups and drop-offs. In *ISTDM 2021*, 2020.
- H. S. Mahmassani, M. Saberi, and A. Zockaie. Urban network gridlock: Theory, characteristics, and dynamics. *Procedia-Social and Behavioral Sciences*, 80:79–98, 2013.
- T. Maruyama and A. Sumalee. Efficiency and equity comparison of cordon-and area-based road pricing schemes using a trip-chain equilibrium model. *Transportation Research Part A: Policy and Practice*, 41(7):655–671, 2007.
- E. Mohareb, S. Derrible, and F. Peiravian. Intersections of jane jacobs' conditions for diversity and low-carbon urban systems: A look at four global cities. *Journal of Urban Planning and Development*, 142(2):05015004, 2016.
- S.-i. Mun, K.-j. Konishi, and K. Yoshikawa. Optimal cordon pricing in a non-monocentric city. *Transportation Research Part A: Policy and Practice*, 39(7-9):723–736, 2005.
- NASEM. The Role of Transit, Shared Modes, and Public Policy in the New Mobility Landscape. Washington, DC: The National Academies Press, 2021.
- NYC Taxi and Limousine Commission. Improving efficiency and managing growth in new york's for-hire vehicle sector. Technical report, 2019.
- E. Özkan and A. R. Ward. Dynamic matching for real-time ride sharing. Stochastic Systems, 2020.
- J. A. Parrott and M. Reich. An earning standard for new york city app-based drivers: Economic analysis and policy assessment, 2018.
- A. C. Pigou. The economics of welfare. Macmillan and Co., London, 1920.

- L. Rayle, D. Dai, N. Chan, R. Cervero, and S. Shaheen. Just a better taxi? a survey-based comparison of taxis, transit, and ridesourcing services in san francisco. *Transport Policy*, 45: 168–178, 2016.
- B. Schaller. Empty seats, full streets: Fixing Manhattan's traffic problem. Technical report, Schaller Consulting, 2017a.
- B. Schaller. Unsustainable? The growth of app-based ride services and traffic, travel and the future of New York City. Technical report, Schaller Consulting, 2017b.
- B. Schaller. The new automobility: Lyft, Uber and the future of American cities. Technical report, Schaller Consulting, 2018a.
- B. Schaller. Making congestion pricing work for traffic and transit in New York City. Technical report, Schaller Consulting, 2018b.
- B. Schaller. Can sharing a ride make for less traffic? Evidence from Uber and Lyft and implications for cities. *Transport policy*, 102:1–10, 2021.
- J. P. Schwieterman and M. Livingston. Uber economics: evaluating the monetary and travel time trade-offs of transportation network companies and transit service in chicago, illinois. Technical report, DePaul University, 2018.
- S. Shaheen. Shared mobility: the potential of ridehailing and pooling. In *Three revolutions*, pages 55–76. Springer, 2018.
- M. H. Shapiro. Density of Demand and the Benefit of Uber. Availabel at http://www.shapiromh.com., 2018.
- H. Sun, H. Wang, and Z. Wan. Model and analysis of labor supply for ride-sharing platforms in the presence of sample self-selection and endogeneity. *Transportation Research Part B: Methodological*, 125:76–93, 2019.
- B. Taylor, R. Chin, M. Crotty, J. Dill, L. Hoel, M. Manville, S. Polzin, B. Schaller, S. Shaheen, D. Sperling, et al. Between public and private mobility: Examining the rise of technology-enabled transportation services. 2016. Special report 319, Committee for Review of Innovative Urban Mobility Services, Transportation Research Board.
- U. US Bureau of Public Roads. *Traffic Assignment Manual for Application with a Large, High Speed Computer*. US Department of Commerce, 1964.
- E. Verhoef, P. Nijkamp, and P. Rietveld. Second-best congestion pricing: the case of an untolled alternative. *Journal of Urban Economics*, 40(3):279–302, 1996.
- E. T. Verhoef. Second-best congestion pricing in general networks. heuristic algorithms for finding second-best optimal toll levels and toll points. *Transportation Research Part B: Methodological*, 36 (8):707–729, 2002.
- D. Vignon, Y. Yin, and J. Ke. Regulating ridesourcing services with product differentiation and congestion externality. *Transportation Research Part C: Emerging Technologies*, 127, 2021.

- H. Wang and H. Yang. E-hailing ride-sourcing systems: A framework and review. 2019.
- X. Wang, F. He, H. Yang, and H. O. Gao. Pricing strategies for a taxi-hailing platform. *Transportation Research Part E: Logistics and Transportation Review*, 93:212–231, 2016.
- K.-I. Wong, S. C. Wong, and H. Yang. Modeling urban taxi services in congested road networks with elastic demand. *Transportation Research Part B: Methodological*, 35(9):819–842, 2001.
- K.-I. Wong, S. C. Wong, H. Yang, and J. Wu. Modeling urban taxi services with multiple user classes and vehicle modes. *Transportation Research Part B: Methodological*, 42(10):985–1007, 2008.
- Z. Xu, Y. Yin, and J. Ye. On the supply curve of ride-hailing systems. *Transportation Research Part B: Methodological*, 132:29–43, 2020.
- C. Yan, H. Zhu, N. Korolko, and D. Woodard. Dynamic pricing and matching in ride-hailing platforms. *Naval Research Logistics (NRL)*, 2019.
- H. Yang and S. Wong. A network model of urban taxi services. *Transportation Research Part B: Methodological*, 32(4):235–246, 1998.
- H. Yang, C. W. Leung, S. Wong, and M. G. Bell. Equilibria of bilateral taxi–customer searching and meeting on networks. *Transportation Research Part B: Methodological*, 44(8):1067–1083, 2010.
- H. Yang, J. Ke, and J. Ye. A universal distribution law of network detour ratios. *Transportation Research Part C: Emerging Technologies*, 96:22–37, 2018.
- H. Yang, X. Qin, J. Ke, and J. Ye. Optimizing matching time interval and matching radius in on-demand ride-sourcing markets. *Transportation Research Part B: Methodological*, 131:84–105, 2020.
- J. J. Yu, C. S. Tang, Z.-J. Max Shen, and X. M. Chen. A balancing act of regulating on-demand ride services. *Management Science*, 66(7):2975–2992, 2020.
- L. Zha, Y. Yin, and H. Yang. Economic analysis of ride-sourcing markets. *Transportation Research Part C: Emerging Technologies*, 71:249–266, 2016.
- L. Zha, Y. Yin, and Z. Xu. Geometric matching and spatial pricing in ride-sourcing markets. *Transportation Research Part C: Emerging Technologies*, 92:58–75, 2018.
- K. Zhang and Y. M. Nie. To pool or not to pool: Equilibrium, pricing and regulation. *Transportation Research Part B: Methodological (in press)*, 2021.
- K. Zhang, H. Chen, S. Yao, L. Xu, J. Ge, X. Liu, and Y. M. Nie. An efficiency paradox of uberization. Availabel at: SSRN 3462912 (Accessed: 2019-10-15), 2019.
- R. Zhang and M. Pavone. Control of robotic mobility-on-demand systems: a queueing-theoretical perspective. *The International Journal of Robotics Research*, 35(1-3):186–203, 2016.
- X. Zhang and H. Yang. The optimal cordon-based network congestion pricing problem. *Transportation Research Part B: Methodological*, 38(6):517–537, 2004.

A Notations

Table 1: List of notations

| Variable | Description | Unit |
|---|--|---------|
| A_i | area of zone i | sqmi |
| w_{ij}^s | solo passenger wait time from zone i to zone j | hr |
| $w^s_{ij} \ w^p_{ij}$ | pooling passenger wait time from zone i to zone j | hr |
| Λ_i | vacant vehicle density in zone i | /sqmi |
| Π_i^s | solo waiting passenger density in zone i | /sqmi |
| $\mid \Pi_{ij}^{p} \mid$ | pooling waiting passenger density for trips from zone i to zone j | /sqmi |
| $\Pi_i^{	ext{eff}}$ | effective waiting passenger density in zone <i>i</i> | /sqmi |
| v_{ij} | traffic speed of trips from zone <i>i</i> to zone <i>j</i> | mph |
| $v_f^{''}$ | free-flow traffic speed | mph |
| C_p | capacity of arterial roads between zones | /hr |
| k' | coefficient of matching efficiency | /sqmi |
| b | coefficient of pooling efficiency | _ |
| κ | approximation parameter in function of w_{ij}^p | /sqmi |
| δ | detour ratio of road network | _ |
| D_{ii}^0 | total demand rate from zone <i>i</i> to zone <i>j</i> | /hr |
| $Q_{ij}^{s} (Q_{ij}^{p})$ | solo (pooling) demand rate from zone i to zone j | /hr |
| Q_{ij} | background traffic flow from zone <i>i</i> to zone <i>j</i> | /hr |
| D_{ij}^{0} $Q_{ij}^{s} (Q_{ij}^{p})$ \bar{Q}_{ij} $f_{ij}^{s} (f_{ij}^{p}, f_{ij}^{t})$ | trip fare of solo rides (pooling rides, transit) from zone <i>i</i> to zone <i>j</i> | \$ |
| $	au^s_{ij} (au^p_{ij}, 	au^t_{ij})$ | average trip duration of solo rides (pooling rides, transit) from zone i to zone j | hr |
| $	au_{ij}^r \ (au_{ij}^0)$ | vehicle relocation time (baseline vehicle travel time) from zone i to zone j | hr |
| $d_{ij}^s (d_{ij}^p)$ | average trip distance of solo rides (pooling rides) from zone i to zone j | hr |
| $\varepsilon_{ij}^{s}\left(\varepsilon_{ij}^{p} ight)$ | distance-independent trip duration of solo rides (pooling rides) from zone i to zone j | hr |
| $u_{ij}^s (u_{ij}^p, u_{ij}^t)$ | general cost of solo rides (pooling rides, transit) from zone <i>i</i> to zone <i>j</i> | \$ |
| $ \bar{u}_{ij} $ | expected saving of a trip from zone <i>i</i> to zone <i>j</i> due to switching from transit to ride-hail service | \$ |
| $\mid \nu \mid$ | value of time | \$/hr |
| θ | Mode choice uncertainty | /\$ |
| $\zeta^p(\zeta^t)$ | relative disutility of pooling (transit) trips | \$/trip |
| S_0 | potential supply | 1 |
| N_i | fleet size (number of drivers in operation) in zone <i>i</i> | |
| V_i | vacant vehicle time in zone <i>i</i> | hr |
| X_i | difference between outbound and inbound occupied vehicle flow of zone i | /hr |

| $X_i^+(\hat{X}_i^+)$ | (approximated) vehicle relocation flow to zone i | /hr |
|---|---|-------|
| $\rho_i \ (\bar{\rho}_i, \rho_i^{\text{jam}})$ | ride-hail (background, jam) vehicle density in zone <i>i</i> | /sqmi |
| z_{ij} (\bar{z}_{ij}) | ride-hail (background) vehicle flow from zone i to zone j | /hr |
| γ | approximation parameter in function of \hat{X}_i^+ | |
| \tilde{e}_0 (\bar{e}_0, \bar{e}_0) | random (upper and lower bounds of) reservation rate | \$/hr |
| e | driver's earning rate | \$/hr |
| η | compensation rate (payment per unit occupied time) | \$/hr |
| C_{ij}^{s} | congestion fee on solo ride from zone i to zone j | \$ |
| $\begin{bmatrix} c_{ij}^s \\ c_i^d \end{bmatrix}$ | congestion fee on relocation vehicles to zone <i>i</i> | \$ |
| μ_i | vehicle occupancy rate in zone <i>i</i> | |
| T | tax revenue | \$ |

B Data

The default values of the parameters used in numerical experiments are reported in Table 2. Most of them are estimated from empirical data collected in the City of Chicago in September 2019, including the TNC data¹², the ridership data from Chicago Transit Authority¹³ and traffic speed data¹⁴.

On the demand side, the total passenger demand for public transport is estimated as the sum of ride-hail and transit ridership. The OD demand pattern is set according to the pattern revealed from the ride-hail trips. In addition, we estimate the trip distance d_s and d_p , as well as the additional travel time ε_s and ε_p , from the TNC data. The transit trip duration is estimated using Goggle Map API. The transit fare f_t and the relative disutility of transit ζ^t are set based on Schwieterman and Livingston (2018). Specifically, ζ^t is measured as proportional to the travel time, i.e., $\zeta^t = z\tau_{ij}^t$. The relative disutility of pooling is set as $\zeta^p = \$0.6/\text{trip}$ according to recent empirical studies (Lavieri and Bhat, 2019; Alonso-González et al., 2021). The passengers' value of time ν is set according to the value of business trips reported in US Bureau of Labor Statistics¹⁵, adjusted to 2019 US dollar value.

On the supply side, the minimum reservation rate \bar{e}_0 is set to be minimum wage rate in the U.S, i.e., \$7.25/hr. The maximum reservation rate \bar{e}_0 is set such that the average reservation rate is \$19.31/hr, the mean hourly wage rate for the occupational group "Transportation and material moving" in the Chicago area¹⁶. The TNC data also include the number of trips served by each registered driver, which helps estimate the potential supply.

¹² Available at https://data.cityofchicago.org/Transportation/Transportation-Network-Providers-Trips/ m6dm-c72p

¹³Available at https://www.transitchicago.com/ridership/

¹⁴ Available at https://data.cityofchicago.org/Transportation/Chicago-Traffic-Tracker-Congestion-Estimates-by-Se/n4j6-wkkf

 $^{^{15}}$ Available at https://www.transportation.gov/office-policy/transportation-policy/guidance-value-time.

¹⁶Available at https://www.bls.gov/regions/midwest/news-release/occupationalemploymentandwages_chicago.htm.

As for the congestion model, we take the free-flow speed v_f and jam density from Mahmassani et al. (2013), who conduct dynamic traffic simulations on a Chicago downtown road network. Note that the jam density reported in Mahmassani et al. (2013) is lane density. To transform it into space density ρ_{jam} , we multiply the value with road density estimates derived in Mohareb et al. (2016). The aggregate road capacity C_p is estimated according to Greenshield's model, i.e., $C_p = v_f \rho_{\text{jam}}/4$. The background traffic is back-calculated from Eqs. (5a) and (5b) using the observed traffic speed and ride-hail trip number. The travel speed without ride-hail vehicles are computed from the same equations while setting ride-hail vehicle flows as zero.

Finally, parameters used in the matching model (i.e., δ , k, b and κ) are taken from Zhang and Nie (2021).

Table 2: Default value of parameters in numerical experiments.

| Parameter | Unit | Default value | |
|--|------------------------|---------------|---|
| Total demand | \mathbf{D}_0 | pax/hr | $34440 \times \begin{bmatrix} 0.18 & 0.23 \\ 0.21 & 0.38 \end{bmatrix}^*$ |
| Average solo trip distance | | mi | [2.6746 3.6353] 3.7550 1.5392] |
| Average pooling trip distance | | mi | [3.8519 4.1357] 4.2476 2.0211] |
| Distance-independent trip duration of solo rides | | hr | 0.1 |
| Distance-independent trip duration of solo rides | | hr | 0.15 |
| Average transit trip duration | $oldsymbol{	au}_t$ | hr | $ \left[\begin{array}{cc} 0.34 & 0.48 \\ 0.47 & 0.31 \end{array} \right] $ |
| Transit trip fare | | \$/ride | 2.69 |
| Passengers' value of time | | \$/hr | 27.69 |
| Relative disutility of transit per unit travel time | | \$/hr | 6.92 |
| Relative disutility of pooling | | \$/trip | 0.6 |
| Mode choice uncertainty | | | 1 |
| Minimum reservation rate | | \$/hr | 7.25 |
| Maximum reservation rate | | \$/hr | 31.37 |
| Potential supply | | veh | 15785 |
| Free-flow speed | v_f | mph | 40 |
| Jam density | $oldsymbol{ ho}_{jam}$ | veh/sqmi | [2000 3000] 3000 4000] |
| Aggregate road capacity | C_p | veh/hr | 30000. |
| Background traffic | $ar{Q}$ | veh/hr | [81219 44034] 43055 73690] |
| Traffic speed without ride-hail vehicles | $ar{m{v}}_0$ | mph | [25.4330 23.5815 [24.4450 20.4262 |
| Default traffic speed in MO pricing without congestion model | | mph | $\left[\begin{array}{cc} 25 & 22\\ 23 & 19 \end{array}\right]$ |
| Detour ratio of road network | | | 1.3 |
| Matching efficiency | | /sqmi | 0.16 |
| Pooling efficiency | | | 0.05 |
| Approximation parameter | | | 4 |
| Zone area | A | sqmi | [22.3, 6.4] |

^{*} All parameters in vector form follow index {0: PA; 1: CBD} and those in matrix form follow index {(0,0): peripheral; (0,1): inbound; (1,0): outbound; (1,1): central}.